UNIVERSIDADE FEDERAL DE SANTA CATARINA
PROGRAMA DE PÓS-GRADUAÇÃO EM ENGENHARIA
MECÂNICA

Cauê Corrêa da Silva

MANUFACTURING AND CHARACTERIZATION OF ALUMINIUM-NICKEL MATRIX COMPOSITES

Florianópolis
2015

Cauê Corrêa da Silva

MANUFACTURING AND CHARACTERIZATION OF ALUMINIUM-NICKEL MATRIX COMPOSITES

Dissertação submetida ao Programa de Pós-Graduação em Engenharia Mecânica da Universidade Federal de Santa Catarina para a obtenção do Grau de Mestre em Engenharia Mecânica.

Orientador: Prof. Márcio C. Fredel, Dr.-Ing.
Coorientador: Prof. Ulrich Tetzlaff, Dr.-Ing.

Florianópolis
2015

Cauê Corrêa da Silva

MANUFACTURING AND CHARACTERIZATION OF ALUMINIUM-NICKEL MATRIX COMPOSITES

Esta Dissertação foi julgada adequada para obtenção do Título de "Mestre em Engenharia Mecânica" e aprovada em sua forma final pelo Programa de Pós-Graduação em Engenharia Mecânica.

Florianópolis, 17 de Dezembro de 2015.

_____
Prof. Armando Albertazzi Gonçalves Jr., Dr.
Coordenador do Curso

_____
Prof. Márcio Celso Fredel, Dr.-Ing. – Orientador
Universidade Federal de Santa Catarina

_____
Prof. Ulrich Tetlzaff, Dr.-Ing. – Coorientador
Technische Hochschule Ingolstadt

Banca Examinadora:

_____
Prof. Márcio Celso Fredel, Dr.-Ing. – Orientador
Universidade Federal de Santa Catarina

_____

Prof. Carlos Augusto Silva de Oliveira, Dr.
Universidade Federal de Santa Catarina

_____

Prof. Carlos Enrique Niño Bohórquez, Dr.
Universidade Federal de Santa Catarina

_____

Prof. Guilherme Mariz de Oliveira Barra, Dr.
Universidade Federal de Santa Catarina

ACKNOWLEDGEMENTS

*"The real voyage of discovery
consists not in seeking new landscapes,
but in having new eyes."*
(Marcel Proust)

ABSTRACT

The present work describes the designing of a manufacturing process for the production of aluminum matrix composites reinforced with carbon fibers. The matrix was chosen to be an interlayering of aluminum foils and nickel mesh stripes, cold rolled with 70% of thickness reduction, being then submitted to different heat treatments, of which immersion in pure aluminum melt was found to be the most promising. Microstructure and composition of the samples were analyzed with scanning electron microscopy, energy-dispersive X-ray spectroscopy, X-ray diffractography and microhardness test, whose results showed the presence of remaining nickel and intermetallic compounds formed during the processing, namely Ni_2Al_3 and $NiAl$, agreeing with studies on reactive diffusion found in the literature. Furthermore, composites were produced by incorporating nickel-coated carbon fibers to the manufacturing process, being evaluated the effect of the fibers addition to the material with scanning electron microscopy, energy-dispersive X-ray spectroscopy, X-ray diffractography and fiber content estimation via image binarization. Intermetallic phases were also present in the microstructure of the composites, nevertheless in smaller extent and in an aluminum matrix. Bond between matrix and fibers was found to be strong, since no fiber pull out took place. Performed fiber content analysis showed that the optimum fiber volume content is between 15% and 40%. Mechanical properties of both without and with fibers materials were assessed through 4-point bending tests, having their fracture surface analyzed afterwards.

Keys words: aluminum matrix composites; carbon fibers; processing; intermetallics

RESUMO

O presente trabalho descreve o desenvolvimento de um processo de fabricação para a produção de compósitos de matriz de alumínio reforçados com fibras de carbono. O material escolhido para a matriz era constituído por camadas intercaladas de folhas de alumínio e malha de níquel, laminadas a frio com 70% de redução de espessura, sendo então submetidos a diferentes tratamentos térmicos, dentre os quais imersão em fundido de alumínio mostrou-se o mais promissor. A microestrutura e a composição das amostras foram analisadas com microscopia eletrônica de varredura, espectroscopia dispersiva de raios-X, difratografia de raios-X e testes de microdureza, cujos resultados mostraram a presença de níquel remanescente e compostos intermetálicos, Ni_2Al_3 e $NiAl$, coincidindo com estudos sobre difusão reativa encontrados na literatura. Além disso, compósitos foram produzidos através da incorporação de fibras de carbono revestidas com níquel ao processo de fabricação, sendo avaliados os efeitos da adição de fibras ao material com microscopia eletrônica de varredura, espectroscopia dispersiva de raios-X, difratografia de raios-X e estimativa do teor de fibras através de binarização de imagens. Fases intermetálicas também estavam presentes na microestrutura do compósito, entretanto em menor quantidade e em uma matriz de alumínio. A adesão entre matriz e fibras foi avaliada como sendo alta, visto que não ocorreu o fenômeno de *pull out* das fibras. As análises de teor de fibra mostraram que o volume de fibras ótimo encontra-se entre 15% e 40%. Tanto propriedades mecânicas do material sem fibra, quanto do com fibra, foram aferidos com teste de flexão em 4 pontos, posteriormente tendo sua superfície de fratura analisada.

Palavras-chave: compósitos de matriz de alumínio; fibras de carbono; processamento; intermetálicos

FIGURE INDEX

TABLE INDEX

ABBREVIATIONS AND ACRONYMS LIST

GRP – Glass reinforced plastics
CFRP – Carbon-fiber reinforced plastics
PTFE – Polytetrafluoroethylene
FRP – Fiber-reinforced plastics
WHIPOX – Wond highly porous oxide composite
Ti-MMC – Titanium metal matrix composites
Ti-Al – Titanium aluminide
C/SiC – Carbon fiber reinforced silicon carbide
CMC – Ceramic matrix composites
PMC – polymer matrix composites
MMC – metal matrix composites
Al_2O_3 – aluminum oxide
ZrO_2 – zirconium dioxide
PAN - poly(acrylonitrile)
Al_2O_3-SiO_2 – mullite
SiC – silicon carbide
Si_3N_4 – silicon nitride
B_4C – boron carbide
AlN – aluminum nitride
TiC – titanium carbide
C/C – carbon-fibers-reinforced carbon-matrix composites
$TiAl_3$ – titanium aluminide
$NiAl_3$ – nickel aluminide
NiAl – nickel aluminide
Ni_3Al – nickel aluminide
TiB_2 – titanium boride
VLS – vapor-liquid-solid for processing
CVD – chemical vapor deposition
PCS – polycarbosilane
SEM – scanning electron microscope
SE – secondary electrons
BSE – back-scattered electrons
EDX – energy-dispersive X-ray spectroscopy
XRD – X-ray diffractography

SYMBOL LIST

l_c – critical fiber length
σ_{Bf} – fibers ultimate tensile strength
d_f – fiber diameter
τ_B – matrix shear strength
G – Gibbs free energy
H – enthalpy
T – temperature
S – entropy
X – molar fraction
X_A – molar fraction of element A
X_B – molar fraction of element B
ΔG_{mix} – variation of Gibbs free energy due to mixture
ΔH_{mix} – variation of enthalpy due to mixture
ΔS_{mix} – variation of entropy due to mixture
X^0 – overall compositionof the system
ΔG^a – activation free energy barrier
k – Boltzmann's constant
E – elastic modulus
ΔP – variation of load
$\Delta \delta$ – variation of deflection

TABLE OF CONTENTS

1 INTRODUCTION

Composites arose to face conditions in which neither metals, nor ceramic, nor polymers by themselves could. The variety of matrices materials and reinforcements materials and shapes, as well as the processing routes for bringing these phases together, enables virtually endless possibilities of combinations, consequently properties that can be tailored[1-5].

When it comes to materials selection, metals present many advantages to be used as matrix in composites, because, generally, they are processable through machining, casting, powder metallurgy, mechanical working, have high toughness, etc. Aluminum is widely used as composite matrix, due to its high specific mechanical properties, processability, possibility of having properties improved through alloying, among other features. Aluminum is very often reinforced with particles or short fibers, to increase its wear resistance and specific mechanical properties, but seldom with long fibers, due to the issues on their processing, such as orientation and distribution. As carbon fibers have the highest specific tensile strength and elastic modulus among the fibers, it is of interest to reinforce aluminum or aluminum alloys with them, producing a composite with high specific mechanical properties and relatively high operation temperature[1-5,11,20-22].

1.1 Main objective

The present work has as its main goal, to develop a feasible manufacturing process of aluminum matrix composites reinforced with carbon fibers.

1.2 Specific objectives

- Define a suitable processing and heat treatment for the matrix material
- Analyze formed phases in the material after treatment
- Incoporate carbon-fiber reinforcement in the processing route
- Evaluate microstructural features of the composite
- Assess and compare mechanical properties of both materials with and without fibers

2   LITERATURE REVIEW

2.1   Composites

The constant research and development towards improving strength, toughness, wear and corrosion resistance, among other properties, of classical engineering materials has found its borders decades ago. In order to reach new goals and open new fields in science and technology, there are requirements that are not fulfilled by metals, ceramics, or polymers alone. From such requirements, the need of combining properties of the classical group of materials arose[1-3].

Since thousands of years composites are already available in nature, considering that wood, for example, allies the good strength and stiffness of cellulose fibers embedded in polysaccharide lignin, as well as produced by mankind, which started using mud bricks reinforced with straw or even horse hair[1-5]. Nevertheless, the industry of high performance composites was initiated with the enabling of large scale production of fiberglass and it has been widespread with the invention of carbon fibers[5], as well as boron and ceramic fibers.

Generally, composites are the combination of two or more materials or material phases, intending to enable the use of their best properties and simultaneously reinforcing their weaknesses. The bulk constituent in a composite material is called matrix and the component that grants stiffness and/or strength, in most of the cases a discontinuous phase, is referred to as reinforcement[3].

Since centuries steel has been used to reinforce concrete and nowadays metal and metal oxide particles reinforce polymers for a wide range of applications. Ceramic particles are used to reinforce metal brake rotors and cutting tools, providing wear resistance and toughness to the material. Polymeric matrices are reinforced with glass, carbon and other fibers to produce light weight parts with high specific elastic modulus and tensile strength[4-6]. Examples of well-known composites are shown in Fig. 1.
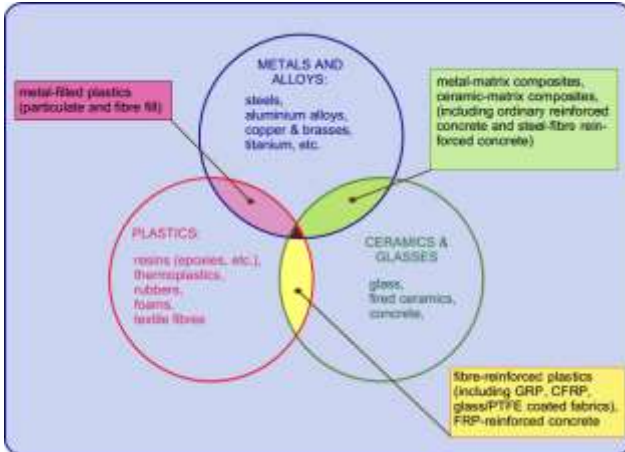
Figure 1 – Combination of materials for the production of a composite [1]

An important boundary condition for materials selection and design is the work temperature, factor that defines the set of materials that can be employed for a determined application. The priority to be fulfilled, is that the selected materials should, of course, present the necessary mechanical properties at the work temperature, lightweight following those in the list of requirements. In Fig. 2 the specific strength, defined as the ratio between strength and density, of commercial high performance materials is shown as a function of temperature, so that these materials are employed at temperatures in which they have the highest specific strength among all[7].
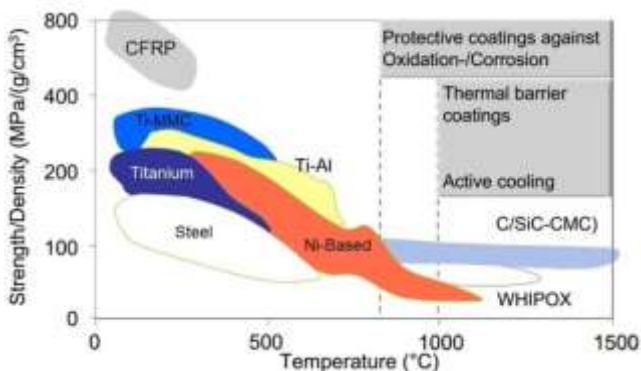
Figure 2 – Specific strength of high performance materials as a function of temperature (Adapted from [7])

Commonly, composites are classified according the material of their matrix, in polymer matrix composites (PMC), metal matrix composites (MMC) or ceramic matrix composites (CMC) and according the aspect ratio, continuity and dispersion of the reinforcement phase[1,3], as shows the scheme in Fig. 3.
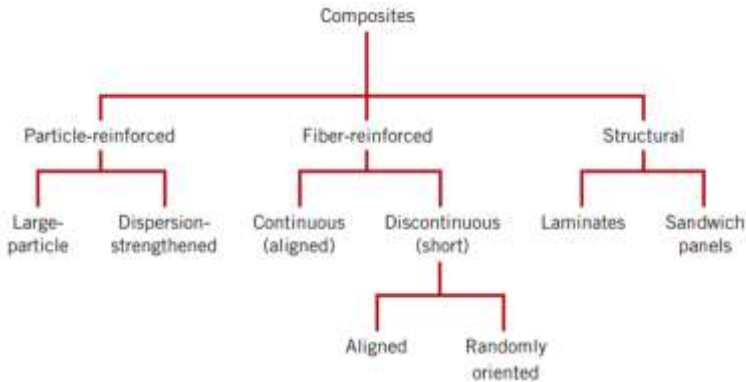
Figure 3 – Classification of various composites types, based on the aspect ratio of the reinforcement phase [4]

2.2   Toughening mechanisms

The effect of reinforcements in a composite is defined by the nature and aspect ratio of the reinforcement, by the nature of the matrix and by the interphase between both. As the reinforcing of materials is firstly driven with the objective of increasing their toughness, the so called toughening mechanisms are the microstructural barriers imposed by the reinforcements, that avoid crack formation or contain its propagation, in both cases by dissipating energy[8]. Based on how crack propagation occurs in the matrix, reinforcements are chosen in order they perform specific toughening mechanisms, such as modulus transfer, prestressing, crack deflection, cracl bridging, pullout, crack shielding, etc[9,10].

2.2.1   Modulus transfer

The fundamentals of reinforcing materials with long fibers rely in a first moment on the modulus transfer mechanism, in which the stress applied in a composite part is carried by the fibers. This mechanism requires fibers with high modulus and strength, being the elastic

modulus at least twice as high as the matrix modulus. Fiber content should be as high as possible, in order to maximize the toughening, but not too high, so that fibers would interact negatively. The strength of the fibers is fully transfered if they break with the matrix during fracture and, for that, fibers should have a minimum length for this mechanism to be effective. Some studies say the fiber length should be 8 times the diameter, while others use the critical fiber length l_c as a parameter, defined as

$$l_c = \frac{\sigma_{Bf}}{\tau_B} \cdot \frac{d_f}{2} \tag{1}$$

where σ_{Bf} is the ultimate tensile strength of the fibers, d_f the diameter of the fibers, τ_B the shear strength of the matrix. If fibers are shorter than the critical length, they are prone to be pulled out, if equal or longer they are supposed to break. This artifice is used for example in metal matrix composites reinforced with ceramic fibers[10,11].

2.2.2 Prestressing

As ceramic materials are much more resistant to compressive than to tensile stresses, ceramic matrix composites are designed to be under residual compressive stress. This can be tailored by stressing fibers in tension, surrounding them with matrix and then releasing the tension of the fibers, making fibers contract and locally inducing the ceramic matrix into compression. Residual compressive strengths can also be generated by processing fibers at high temperature with higher thermal expansion coefficient than the matrix, resulting in compressive residual stresses after the cooling or using fibers with negative thermal expansion coefficent, like aramid or carbons fibers, for applications at high temperatures[10].

2.2.3 Crack deflection

In composite materials, whose bonding between matrix and reinforcement is rather weak, also usually in particle-reinforced composites, crack deflection might be an active toughening mechanism. As the crack propagates through the weakest links in the material, it should be deflected towards the reinforcement/matrix interphases

(Fig. 4). With a proper size and distribution of the reinforcements, this phenomenon should take place subsequently, increasing the crack path and the surface area created by the failure, which, by its turn, requires more energy to be created[8-10].

2.2.4 Crack bridging

If cracks come across reinforcements without leading them to failure, reinforcements are left behind the tip of the crack, linking both created surfaces, leaving residual compression stresses, as shown in Fig. 5a. Ceramic matrix composites reinforced with short or long fibers are designed to enable this mechanism during failure, nevertheless, it can also be identified in metals reinforced with particles. The reinforcement/matrix bonding must be accordingly adjusted for this mechanism to be possible[8,10].

2.2.5 Pullout

The energy required to debond a particle or fiber and then to overcome the friction to open a crack (Fig. 5c) is higher than it would be propagate a crack inside a non-reinforced material. The so called pullout mechanism is often combined with crack bridging (Fig. 5b), usually a feature designed for fiber-reinforced ceramic composites. It can even be enable with adjusted grain size, shape and orientation[8,10].
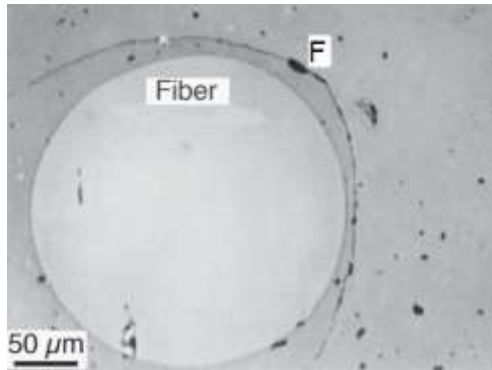
Figure 4 – Crack F, deflected around a Al_2O_3 fiber in a glass-ceramic matrix during a toughness measurement test (Adapted from [12])
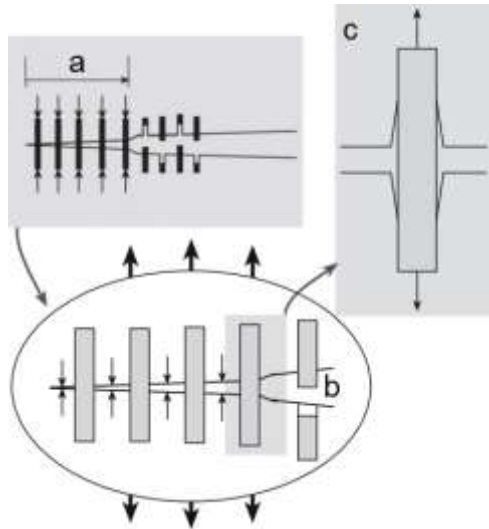
Figure 5 – Fibers retarding crack propagation a) crack bridging b) pulled-out fiber c) fiber being pulled-out (Adapted from [12])

2.2.6 Crack shielding

Crack shielding is a mechanism that develops stress around the crack tip, for example by generating microcracks in the surroundings, reducing the stress at the tip, or by compressing it through a volume increasing transformation of a second phase. With controlled dopping of zirconium dioxide (ZrO_2) with other oxides and a proper heat treatment, ZrO_2 is precipitated in tetragonal phase, which is metastable and can be transformed into monoclinic phase with volume expansion through stress application (Fig. 6)[10].
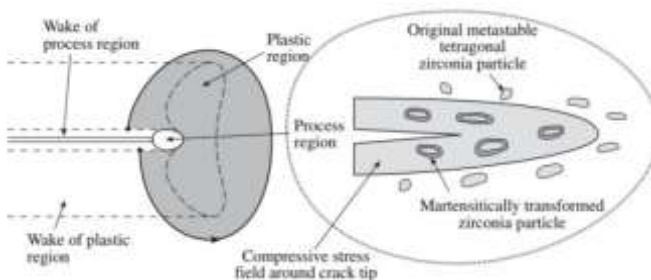
Figure 6 – Crack shielding mechanism induced by phase transformation [12]

2.3   Polymer matrix composites

Polymeric materials offer many advantages for a wide range of manufacturing processes and applications, such as low denisty, ductility, ease of processing and consequently low production cost. Many polymers show high strength-density and elastic modulus-density ratios, i.e. high specific strength and high specific modulus, nevertheless, these properties decrease with the increase of temperature, along with chemical degradation. Chemical degradation is very difficult to be avoided or slowed down over 300°C for most of the polymers, but the temperature-dependent loss of mechanical properties can be decelerate by reinforcing polymers with fibers[1].

For the reinforcement to be effective, adhesion between matrix and fibers should be adequate, so that load can be transferred from the matrix to the fibers, taking the properties of the composite to a higher level than the one of the unreinforced polymer[11].

2.3.1 Matrix

Different polymers can be used as matrix for a PMC, as far as they are ductile and can be processed to produce a proper interface with the reinforcements. Examples are unsaturated polyesters, vinyl esters, diallyl phthalates, methyl methacrylate, epoxides, polyurethanes, phenol formaldehyde and amino resins[11]. The varieaty on chemical compositions and processing routes enables the covering of applications at a wide range of temperatures and solicitations. Properties of the most used polymers as composite matrices are given in Table 1.

Table 1 – Matrices used for advanced polymer composites [13]

Resin family	Typical cure temperature (°C)	Maximum service temperature (°C)	Typical tensile strength (MPa)	Typical elastic modulus (GPa)
Epoxy	175	175	55 – 90	2.6 – 3.4
Phenolic	150	150	7 – 11	0.5 – 1.0
Bismaleimide	190	230	82	4.3
Cyanate	80	175	87	3.2

2.3.2 Reinforcements

2.3.2.1 Glass fibers

Glass fibers are produced by drawing molten glass, initially at 1500°C, in filaments with 5-24 μm diameter, which are quenched to avoid crystallization and protected from oxidation and damaging to maintain the deffect-free surface that results from the processing[1,4]. The only glass used in large scale in the composites industry is the common borosicilate glass, also called E-glass, what is justified by the fact that it has good properties and low production cost[13]. The processing route of fiberglass is shown in Fig. 7, the composition of some fibers classified according their specifics are shown in Table 2 and some of their properties in Table 3.

1. Glass mixture preparation
2. Continuous mixture input
3. Melt tank
4. Heat exchanger
5. Molten glass (approx. 1500°C)
6. Die (Pt-Rh)
7. Sizing
8. Winding
9. Spinning bobbins
10. Glass scrap for reprocessing
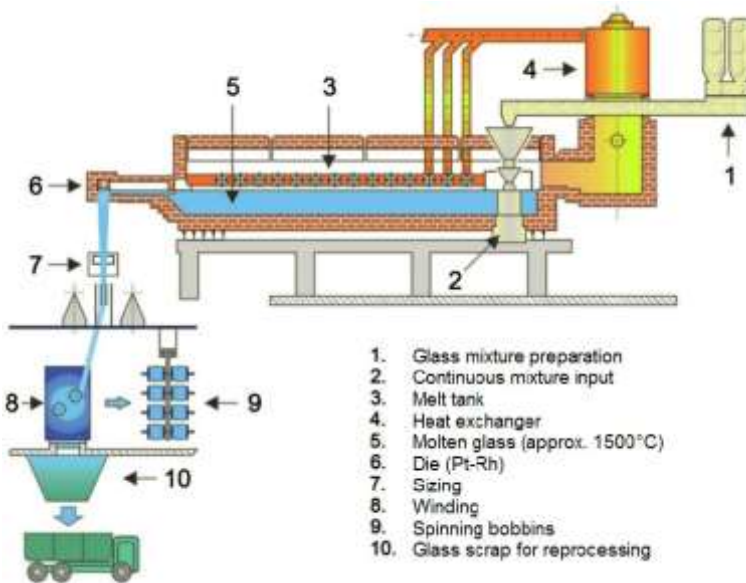
Figure 7 – Illustration of the manufacturing process of glass fibers (Adapted from [13])

Table 2 – Selected properties of commercial glass fibers [13]

Properties	E-glass	ECR	C-glass	AR	R-glass	D-glass
Density (g/cm³)	2.60	2.72	2.52	2.68	2.53	2.14
Tensile strength (MPa)	3400	3445	2400	3000	4400	2500
E-Modulus (GPa)	73	73	70	73	86	55
Elongation to rupture (%)	4.8	4.8	4.8	4.4	4.8	4.8

Table 3 – Chemical composition of commercial glass fibers [13]

Chemical Composition	Polyvalent Glass	Acid Resistant Glass		Alkaline Resistant Glass	High-strength Glass		Glass with good dieletric properties	
Component (wt%)	Type E	ECR	Type C	AR	Type R	Type S	Type D	Quarz
SiO_2	53-54	54-62	60-65	62	60	62-65	73-74	100
Al_2O_3	14-15	9-15	2-6	0.2	25	20-25		
CaO	20-24	17-25	14	5,3	6			
MgO		0-4	1-3	9	10-15	0.5-0.6		
B_2O_3	6-9		2-7			0-1.2	22-23	
Na_2O	0-0.7	0-2	8-19	14.3		0-1.1	1.3	
ZrO_2				17.3				
K_2O							1.5	
Fe_2O_3		0-0.8						
TiO_2		0-4						

2.3.2.2 Aramid fibers

Poly(paraphtelene terephtalamide)s, usually called aramid were thoroughly studied in the 1960s and 1970s, with the objective of replace steel wires used, for example, in tires. Under names like Kevlar™, Nomex™, Twaron™, Teijin™ and others, aramid fibers met applications in the militar industry (proof vests and armors), sports gears, pressure vessels, etc[1,4,13].

The most remarkable properties of aramid fibers are the low density, the lowest among all reinforcement fibers, high tensile strength, high elastic modulus, high impact absorption, negative thermal expansion coefficient, low heat and electricity conductions. Disadvantages that should be considered are humidity absorption and consequent loss of properties, as well as low compressive strength[1,4,13].

2.3.2.3 Carbon fibers

Carbon fibers are fibers that have a very organized graphite-like structure and also some amorphous phase, whose precursors can be, in most of the cases, poly(acrylonitrile), rayon or pitch, being poly(acrylonitrile) (PAN) the most common one. Generally, pitch forms fibers with higher stiffness than PAN, but with lower strength[1,2,4,13].

The transformation process of precursors in carbon fibers requires a lot of time and energy, which is divided in stabilization of the precursor, carbonization, surface treatment, sizing, winding. Being PAN the most used carbon fiber precursor, only its processing will be discussed.

The complete stabilization of PAN-fibers lasts approx. 60 to 120 minutes at temperatures ranging from 200°C up to 300°C under stress. The polymer is oxidized, eliminating water as a by-product. Meanwhile, a pre-orientation of the molecules takes place, making the polymer conducting. This polymer undergoes a cycling heat treatment, forming pyridine rings. After this step, melting the fibers should not be possible, enabling carbonization[13].

Carbonization promotes the clustering of pyridine chains into molecular bands, eliminating hydrogen cyanide and nitrogen. The temperature in this step defines whether the fibers will present high tensile strength (1200°C – 1500°C), intermediate elastic modulus (1500°C – 1800°C) or ultra high elastic modulus (graphitized in a separate step at 3000°C). Both carbonization and graphitization steps are

conducted in a protective atmosphere. The fibers have then their surface treated and are winded[13], as depicted in Fig. 8.

Treatment of the fiber surface has the function of improving the processability for the production of semimanufactured products, improving of the fiber wettability by the composite matrix and optimization of the tenacification mechanisms by the reinforcement. Properties like low density, high tensile strength, high stiffness (Table 4), chemical stability in many media, electric conductivity, thermal stability, biocompatibility and invisibility to X-rays make carbon fibers suitable for a wide range of applications[13]. Polymer matrix composites already gained market and are being used to produce more and more components, like in the structure of the Airbus A380, as shown in Fig. 9.
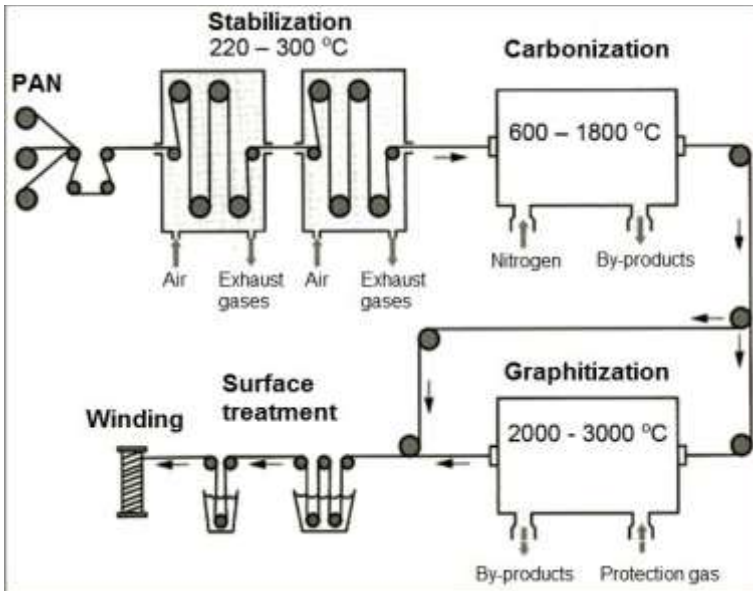
Figure 8 – Carbon fibers production based on PAN-precursors (Adapted from [13])

Table 4 – Examples of comercially available carbon fibers and their properties [13, 14]

Supplier	Trade name	Elastic Modulus (GPa)	Tensile Strength (GPa)	Density (g/cm³)
Toray	Torayca T300	230	3.53	1.76
	Torayca T100G	294	6.27	1.80
	Torayca M60J	588	3.92	1.94
Hexcel	AS4	228	4.07	1.79
	IM9	276	6.00	1.79
	UHM	440	3.73	1.87
Toho Tenax (Tenax®-)	E HTS40 F13	240	4.40	1.77
	E HTS45 E23	240	4.40	1.77
	J UTS50 F13	245	5.10	1.78
	J UMS45 F22	425	4.60	1.83
	J HTS40 A23 MC*	230	2.90	2.70
Nippon	Granoc YS95A	920	3.53	-

*Nickel coated
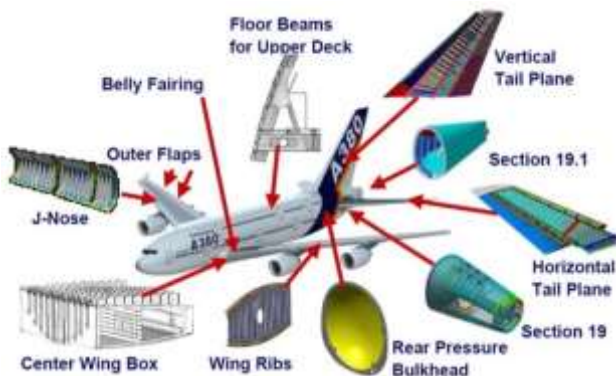
Figure 9 – Structural components made of PMCs in the Airbus A380 [15]

2.3.2.4 Other fibers

In a smaller extension than the glass and carbon fibers, natural, basalt, quartz and ceramic fibers, whose properties and/or cost make them cover also different applications rather than the already cited reinforcements[4,13].

2.4 Ceramic matrix composites

Ceramic materials present very characteristic properties, for example, advantageously high temperature stability, high thermal shock resistance, high elastic modulus, among others. Nevertheless, ceramics are also well known for their brittle behaviour, a macroscopic result of their inability of resisting to crack propagation, which is the main improvement sought with the manufacturing of ceramic matrix composites[16]. Flexural strength and fracture toughness of some ceramics are compared with their composites in Table 5.

2.4.1 Matrix

Matrices used in CMCs are usually the materials already used as structural ceramics, which are divided in oxides, like alumina (Al_2O_3), mullite (Al_2O_3-SiO_2) and zirconia (ZrO_2), or non-oxides, like silicon carbide (SiC), silicon nitride (Si_3N_4), boron carbide (B_4C) and aluminium nitride (AlN). For long-fiber-reinforced composites, carbon is the most used matrix material[16,17].

Table 5 – Comparison between engineering ceramics with and without reinforcement [13]

Material	Flexural Strength (MPa)	Fracture toughness (MPa·m$^{1/2}$)
Al_2O_3	358	4-5
Al_2O_3 – 30wt% TiC_p	638	4,5
Al_2O_3 – 30vol% SiC_w	660	8,6
SiC	380	4,6
SiC – 16vol% TiB_{2p}	478	6,8 – 8,9
Si_3N_4	700	6
Si_3N_4 – 30vol% SiC_p	885	4,9
Si_3N_4 – 30vol% 0,5 μm SiC_w	970	6,4

2.4.2 Reinforcements

Particle-reinforced ceramic composites are normally manufactured through powder sintering routes, requiring aid of hot pressing or hot isostatic pressing for particle content over 15-20 vol%. Particles are typically equiaxed and of carbides (SiC, TiC, B_4C) and other very hard ceramics, as well as dopped ZrO_2, designed to increase the composite toughness through the crack shielding mechanism[13].

Reinforcing ceramic materials with deffect-free short fibers (whiskers) has shown success not only on increasing strength and toughness, but also on maintaining these properties at high temperatures. Composites reinforced with 10 vol% whisker content should be hot pressed or liquid-phase sintered, in order to obtain a dense microstructure[13].

Carbon-fibers-reinforced carbon-matrix composites (C/C) were the first CMCs to be empolyed in the aerospacial industry, as they present high mechanical properties and temperature resistance in non-oxidative atmospheres, driving the research on environmental barrier coatings. Carbon has also found use as reinforcement for SiC, but both C/C and carbon-fiber-reinforced SiC (C/SiC) are produced through high cost processes, what restricts their applications to functions for which metals are too heavy and/or cannot resist the thermomechanical solicitations, for example, high performance brake disks (Fig. 10). Even though oxides reinforced with oxide fibers do not show such a high stiffness nor strength as C/C or C/SiC, they are stable at high temperature in air and/or water vapour atmospheres, enabling their application in stationary gas turbines, for example[16,17].
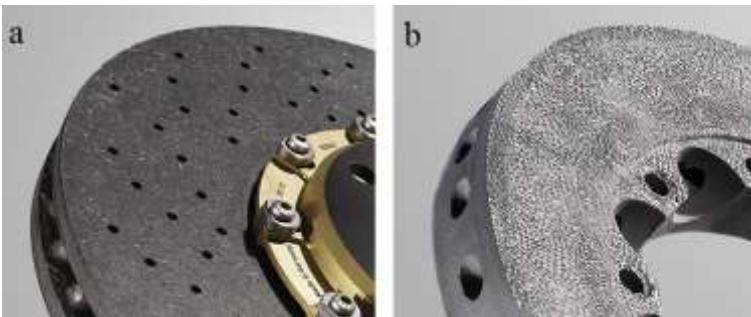
Figure 10 – Ceramic composites brake discs produced via hot pressing a) C/SiC b)C/C [18]

2.5 Metal matrix composites

For engineering purposes, metals are usually preferred over ceramics and polymers due to their strength, toughness, workability, etc. Yet, the development of science and industry required more performance than that of metals or other materials alone. In order to increase strength, elastic modulus, creep, fatigue and wear resistance, as well as other properties, manufacturing processes for reinforcing metals with ceramic particles, ceramic, carbon, boron or refractory metal fibers started being studied and developed. The diversity in metal alloys and the several reinforcement variables that can be controlled, such as size, shape, distribution, etc, enable the production of uncountable different metal matrix composites, covering applications in many industries, like recreational, transport, automobilistic, aerospacial and others[19-22].

2.5.1 Matrix

2.5.1.1 Aluminum alloys

Aluminium's low melting point (compared to other metals), low density, high corrosion resistance and ability of being strengthened by alloying, heat treatment and/or cold working makes it a very versatile material, which can be processed through many different routes with different reinforcements, such as infiltration or reaction infiltration of preforms, squeeze casting, powder metallurgy, extrusion, thixocasting and many others[21-23].

Classification of aluminium alloys is firstly divided into wrought (laminated, extruded, forged, stamped and other forms) and cast alloys, the latest having lower melting point and lower strength. In both categories there are alloys that can be precipitation heat-treated, or age-hardened, and alloys that cannot. Alloys, which can have their mechanical properties increased through heat treatment, are basically submitted to a heat treatment, either simply cooling down or a solution heat treatment, during the shaping process or after it and then are aged naturally (at room temperature) or artificially (at temperatures above room temperature). Non-heat-treatable alloys are commonly cold worked and eventually stabilized by heat produced during the fabrication or by a low temperature heat treatment or annealed[23,24].

2.5.1.2 Titanium alloys

Due to the density range of its alloys, between 4.3 g/cm³ and 5.1 g/cm³, and the elastic modulus varying from 80 to 130 GPa, titanium has become a very useful in applications in which high strength and weight saving are priorities. Not only that, titanium has a relatively high melting point, 1672°C, and it presents good strength at elevated temperatures. These features make the investments on extraction and processing worthy, since titanium is seldom found in high concentrations in minerals and it is more easily shaped through hot processes, because pure titanium presents hexagonal close packed crystalline structure at room temperature and body-centered cubic at over 882°C[22,25].

Titanium alloys are primarily divided into α, near-α, α+β, and metastable β alloys. For uses in which high corrosion resistance is the highest priority, α alloys are used, presenting good cold formability and low strength, compared to other Ti-alloys. Near-α alloys combine excellent creep behavior with high strength, being employed at temperatures up to 550°C. For high strength and toughness, α+β alloys are hot worked, breaking the structure of the β phase and dispersing it in a very fine form. Among the α+β alloys is the most used Ti-alloy, Ti-6Al-4V, largely used in the aerospace industry. Based on a complex microstructure, β alloys can have their properties tailored and become thin foils or high strength and high toughness components, having their possibilities limited by low weldability and poor oxidation resistance though[25].

2.5.1.3 Nickel alloys

The ability of solubilizing several elements, like copper, iron, chromium, molybdenum, tungsten, aluminium, manganese and vanadium, in large contents, gives the chance of designing nickel alloys with unique microstructures and precipitation behaviors and, consequently, unpaired corrosion resistance and mechanical properties over many combinations of environments and temperatures[13,26].

Nickel-copper alloys are ideal for applications with high flow velocity and moderately corrosive environment and the precipitation-hardenable ones can operate up to 600°C, being used for marine and oil and gas applications. Nickel-iron alloys have high magnetic permeability, making components for transformers, low-frequency transducers, etc. Nickel-silicon alloys are used to handle hot or boiling sulfuric acid, as well as nitric and sulfuric acid mixtures. Nickel-chromium-iron alloys are used in thermal and chemical processes,

automotive industry and others. Other newer developments comprise small amounts of other elements in their composition, so that the atoms of different sizes retard diffusion by substituting matrix atoms, as in the alloys for jet engine tubine blades[13,22,26].

2.5.1.4 Other metals

Among all the metallic elements of the periodic table, many can be and are used as matrices for composite materials. Worldwide hard metal cutting inserts are used, whose constitution is a carbide (originally tungsten carbide) in a cobalt matrix. For functional, i.e. not structural, components, strength and toughness are not priorities, but thermal or electric properties must be fulfilled. Copper, silver and niobium are, for example, used in superconductors[13,22].

2.5.1.5 Intermetallics

New approaches in the research and development of composites are working on manufacturing intermetallic matrix composites. Intermetallics are compounds formed by two or more different metals, combined to each other with covalent or ionic bondings. The nature of their bondings and, for the ones who present it, the crystalline structure of the intermetallic compounds provide them with a very particular set of interesting properties for many applications. Generally lightweight, highly resistant to oxidation, stiff, intermetallics maintain their high mechanical properties at high temperatures, all of that at the cost of a poor machinability due to their brittleness at room temperature and the need of very precise composition control for some of them, as for $TiAl_3$ (Fig. 11) and $NiAl_3$ (Fig. 12), so that the compounds do not change their crystal structures[13,22].

Molybdenum disilicide is an intermetallic material used in heating elements since many years, iron silicide is used in high-temperature castings and some silicides are used as coating to protect other materials from oxidation[13]. Little progress has been achieved towards silicide matrix composites, but the use of these materials as coatings for refractory metals and alloys is so far successful[28].

Much effort was invested on understanding the crystal structure, deformation mechanisms and on the processing of NiAl, an intermetallic compound with outstanding properties at high temperatures, but very brittle and difficult to shape. Due its lower density than nickel alloys and

higher mechanical properties at even higher temperatures, NiAl would be ideal to replace nickel alloys in turbine blades[28].
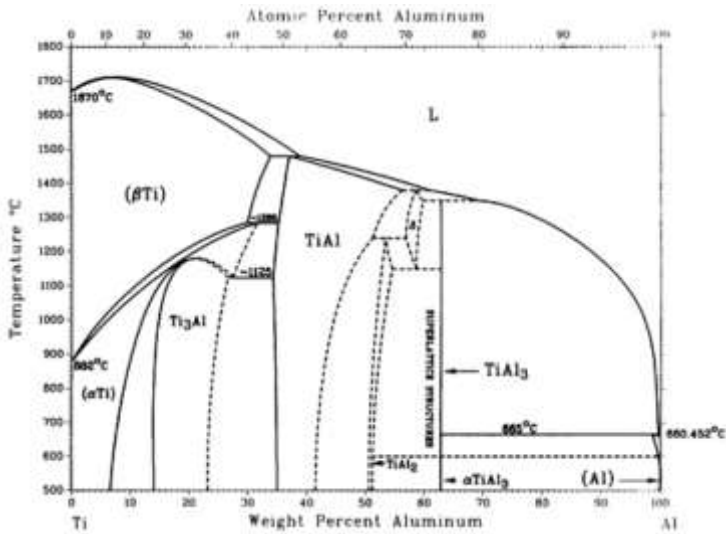
Figure 11 – Ti-Al phase diagram, where TiAl$_3$ can be observed as a line [27]
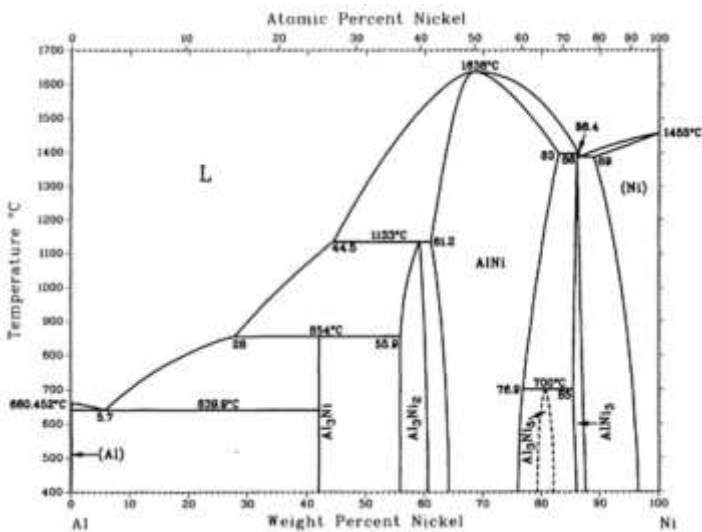
Figure 12 – Al-Ni phase diagram [27]

Despite the difficulties on processing Ni_3Al, interest for applications such as automotive turbochargers, high-temperature dies, hydroturbines, cutting tools, etc., has been enough driving force for experiments, which have shown promising results, such as the investment cast turbocharger rotor in Fig. 13[29].
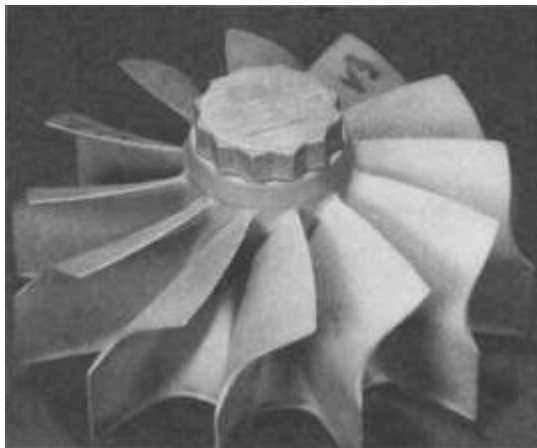
Figure 13 – Investment cast turbocharger made of Ni_3Al [29]

Many processing routes are available for the production of Ti_3Al-based alloys, which are used for support rings, nozzle seals, compressor casings, etc[30].

NiAl had its toughness improved with tungsten, molybdenum or Al_2O_3 fibers or fine dispersed TiB_2 or AlN particles. Improvement in Ni_3Al ductility and ultimate tensile strength was made by alloying it with boron and oxide ceramics, among which the greatest improvement was with reactive sintering of Ni_3Al with B, resulting in 729 MPa ultimate tensile strength and 11.4% ductility. Nevertheless, there are still challenges that must be overcome, for intermetallics and their composites to be realiable and affordable[29].

2.5.2 Reinforcements

As the aim of producing MMCs are weight saving, stiffness improvement, application at higher temperatures than the ones of pure metals, reinforcing materials for metals must clearly present lower density, higher stiffness and temperature resistance than the desired matrix. Based on this premise, ceramic materials, and in a smaller

extension carbon fibers, are the most used reinforcement phase in metal matrix composites, increasing their wear resistance, dimensional stability and creep resistance, etc[21,22].

2.5.2.1 Particles

Since ceramic particles are relatively easy to produce, comparing with other aspect ratios, and its technology is well known from abrasive and sintering industries, they were at the starting point of MMCs production. Ceramic particles provide metallic microstructures with grain boundary pinning, retarding grain growth and consequently increasing temperature resistance, also working as crack path deflectors. An important factor in the designing of composites is the bond strength between matrix and reinforcement, which depends on the nature of both[21,22]. Examples of ceramic materials used as particle reinforcement in MMCs and some properties are listed in Table 6.

Table 6 – Properties of ceramic materials commonly used as reinforcement in MMCs [21]

Property	SiC	Al_2O_3	AlN	B_4C	TiB_2	TiC
Melting point (°C)	2300	2050	2300	2450	2900	3140
E-Modulus (GPa)	480	410	350	450	370	320
Density (g/cm³)	3.21	3.9	3.25	2.52	4.5	4.93
Mohs Hardness	9.7	6.5	-	9.5	-	-
Manufacturer	Wacker Ceramics Kempten	Wacker Ceramics Kempten	H.C. Starck	Wacker Ceramics Kempten	H.C. Starck	Wacker Ceramics Kempten

Little trend has been observed on the effect of the shape of the particles over the composite properties, but studies suggest that flate surfaces are prone to nucleate voids when normal to the applied stress. Concerning the size of the particles, it has been observed that it is more likely for larger particles to initiate a crack, though larger particles are

found to provide a greater increase on toughness. Crack initiation is also favored in regions of high concentration of reinforcement[20].

Particles are very versatile when it comes to processing, because the control over variables such as shape, size distribution, nature, surface characteristics enable a manifold of manufacturing routes as, for example, powder metallurgy, liquid infiltration of preforms, pressure-assisted infiltration (squeeze casting), extrusion, among others[22].

Particle reinforced aluminium matrix composites arouse more interest in a first moment for being lightweight and more easily processed and machined, therefore they are already being employed in many fields, like automotive and high speed trains breaking systems (Fig. 14), fan exit guide vanes, recreational and many others[31,32].
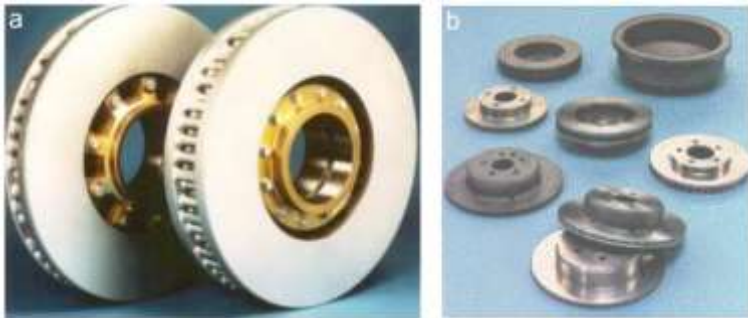
Figure 14 – Aluminium matrix composites brake discs for a) trains b) cars [30]

2.5.2.2 Short fibers and Whiskers

Short fibers are attractive reinforcements because they provide a higher toughness improvement than particles and are less expensive than long fibers, also enabling isotropic reinforcement. Of greater interest are whiskers, which are defect-free short fibers, in general grown through vapor-liquid-solid (VLS) process, or sometimes produced through atomization[20]. Table 7 shows properties of commercial whiskers.

Table 7 – Properties and composition of commercially available whiskers [20]

Trade name	Manufacturer	Composition	Fiber diameter (µm)	Density (g/cm³)	E-Modulus (GPa)	Tensile strength (MPa)
Saffil RF	Saffil	δ-Al_2O_3	1-5	3.3	300	2000
Nextel 440	3M	70 Al_2O_3 28 SiO_2 2 B_2O_3	10-12	3.05	190	2000
SCW #1	Tateho Silicon	β-$SiC_{(w)}$	0.5-1.5	3.18	481	2600
Alborex	Shikoku Chem.	9 Al_2O_3 1 B_2O_3	0.5-1.0	3.0	400	8000

2.5.2.3 Long fibers

The main advantage of using long fibers as a reinforcement is the maximum modulus transfer that can be obtained when fibers are aligned along one axis, ideal in cases of particular high stresses in one direction, or adjusting fibers orientations in more directions, depending on the work solicitations. Long fibers are roughly divided in monofilaments, with diameters ranging from 100 to 150 µm, and multifilaments, with 6 to 20 µm diameters, the latest being used in bundles of 500 to many thousands of filaments[21].

The most used monofilaments are produced through chemical vapor deposition (CVD) of SiC on carbon or tungsten fibers or B exclusively on tungsten fibers[21]. Monofilaments manufacturing is depicted in Fig. 15. Such a processing is expensive and resulting fibers are so far used in special applications, because they present very high tensile strength and can present an elastic modulus just as high as from the monolitic ceramics. Titanium matrix composites reinforced with SiC monofilaments with carbon core (Fig. 16) have been carefully designed[33-35], produced and extensively studied for aerospacial applications (Fig. 17).

Multifilament oxide long fibers with relatively low melting point can be produced by drawing fibers from ceramic molten, but high Al_2O_3-content fibers are produced by sol-gel processing. SiC fibers are produced by controlled pyrolysis of a polycarbosilane (PCS), in which a

SiO$_2$ layer is formed on the surface, improving wettability and consequently adhesion with many metallic matrices[21,22].
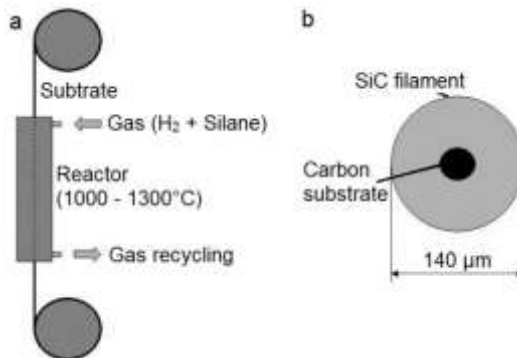
Figure 15 – SiC monofilament a) production and b) cross section (Adapted from [21])
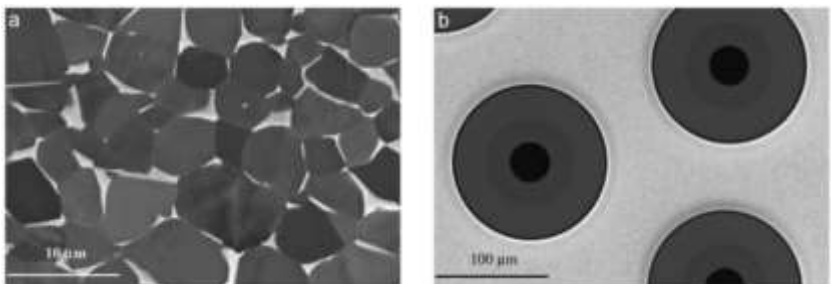
Figure 16 – Titanium matrix composite a) Titanium alloy matrix consisting of α-grains (dark) and β-grains (light) (SEM, BSE) and b) overview on the distribution of SiC fibers in the matrix (SEM, SE) (Adapted from [35])
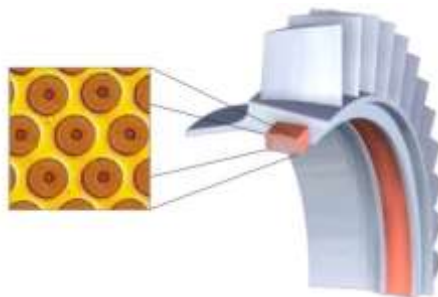
Figure 17 – Application of titanium matrix composites in jet engine components (Adapted from [7])

2.6   Processing of metal matrix composites

The variety of properties of metals and their alloys enables the use of many different approaches for the processing of MMCs, which are usually defined by the type, distribution and, if it is the case, orientation of the reinforcement phase. Regardless of being pressure assisted or not, almost all processing routes of metal matrix composites involve one or more heat treatment steps, either to promote bonding of solid phases through diffusion, or to cast a metal into a reinforcement preform. Yet, the distribution and surface properties of the reinforcement can be also controlled via deposition methods, such as CVD, PVD, plasma spray and others[6,21].

2.6.1   Solid state processing routes

Discontinuous reinforcement phases, i.e. particles or short fibers, are often blended in to composites by incorporating them in metal mixture powders. In order to increase the interaction between matrix and reinforcement, these composite mixtures are mechanically worked via pressing, extruding (Fig. 18), rolling, etc., under vaccum or controlled atmosphere, resulting in higher mechanical properties before and after heat treatment. These routes offer a high control porosity, distribution of reinforcement and some even enable the orientation of short fibers. Disadvantages are that metal powders imply also metal oxide layers around the particles, which must be broken in order to produce a massive composite, besides health and pyrophoricity issues associated with metal and reinforcement particulates. Also, these routes are usually more expensive than liquid state routes[6,21,36].
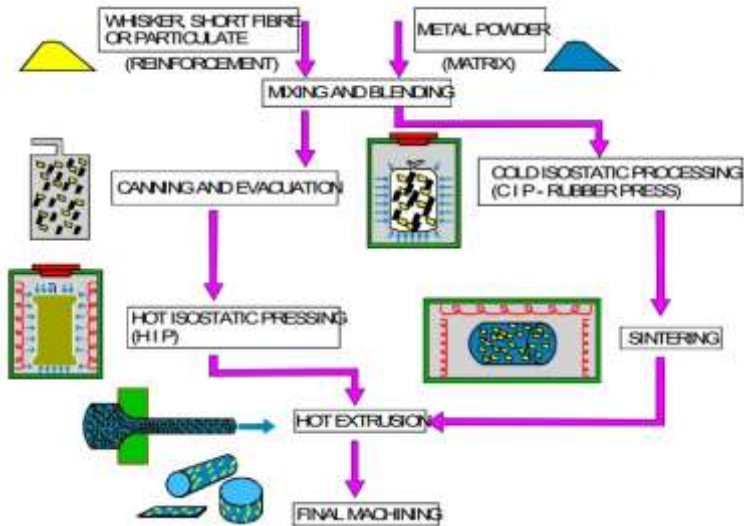
Figure 18 – Powder metallurgical processing route of discontinuosly reinforced MMCs [6]

Long-fiber reinforced composites are very often produced via solid state diffusion bonding, which consists of coating fibers, generally monofilaments, with the matrix metal via PVD, CVD or other deposition method, producing composite foils that are then layed-up and submitted to a consolidation step, under high pressure and temperature (Fig. 19). The coating of fibers enable control of interphase formed with the matrix, gradient of phases formed between fibers and matrix and thus a whole range of properties and applications. These processing methods are important for industries where high mechanical properties are more important than the costs with them associated[6,36].
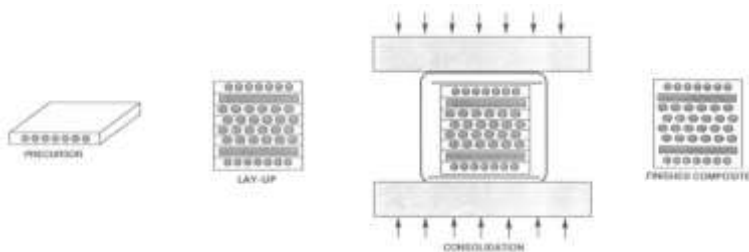
Figure 19 – Diffusion bonding of long-fiber reinforced MMCs (Adapted from [36])

2.6.2 *Liquid state processing routes*

Both powder processing of discontinuously reinforced and diffusion bonding of long-fiber reinforced MMCs can be assisted by liquid phase, namely liquid phase sintering and hot moulding, respectively. However, liquid state processing of MMCs mostly refers to the casting of reinforcement dispersions in molten metal or infiltration of preforms or particles and/or fibers, or fibers arrays[6,36].

Several casting methods of MMCs have been developed, assisted by high pressure, low pressure, centrifugal forces, etc. Among them, squeeze casting has become more popular, by producing fine equiaxed grains and void free, using typically between 70 MPa and 150 MPa of uniaxial pressure. This technique is used for casting of metal mixtures, as well as for infiltration of reinforcement preforms (Fig. 20)[6].
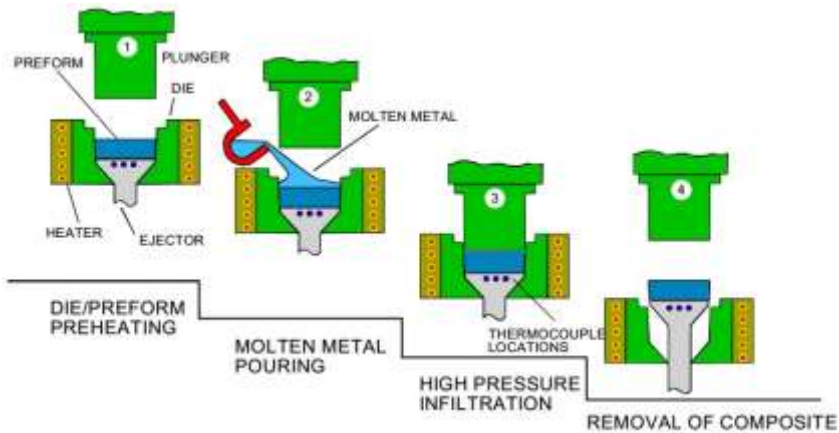
Figure 20 – Squeeze casting infiltration of a discontinuous-reinforcement preform [6]

Liquid metal droplets can also be sprayed with a plasma gun onto wound reinforcement filaments, producing long-fiber reinforced MMCs. Fibers can be pre-coated to ease wettability and prevent reaction between them and the matrix[36].

Casting routes have high potential for near-net-shape manufacturing at relatively low cost, features of high importance in automotive, transportation and other industries. Care must be taken to the same risks of deffect formation as for classical casting, such as remaining porosity, shrinkage, etc[36].

2.6.3   Other processing routes

Other manufacturing processes of MMCs have been developed using varied approaches. Controlled oxidation (for example, the Lanxide process), reaction between ceramic and molten metal (XD-process), nitriding, carburizing and plasma assisted deposition methods are alternative routes, but are used in a smaller extent due to their cost and complexity compared to the properties of the resulting composites[6,36].

3   MATERIALS AND METHODS

3.1   Materials selection

For the manufacturing of a multiphase aluminium matrix material were used aluminium foils (EDEKA AG & Co. KG, Germany, Fig. 34), acquired as a 30 m-long, 0,3 m-wide and 13 µm-thick roll, and nickel mesh (HAVER & BÖCKER OHG, Germany), obtained as a 2,5 m-long, approximately 1 m-wide, whose wires have a diameter of around 55 µm and a nominal mesh aperture of 80 µm (Fig. 35). Reinforced samples were produced by introducing nickel-coated carbon fibers (HTS40 A23, Toho Tenax Europe GmbH, Germany, Fig. 36) in the manufacturing process of the aluminium matrix composite material.

Figure 21 – Aluminium foils used for sample production [40]
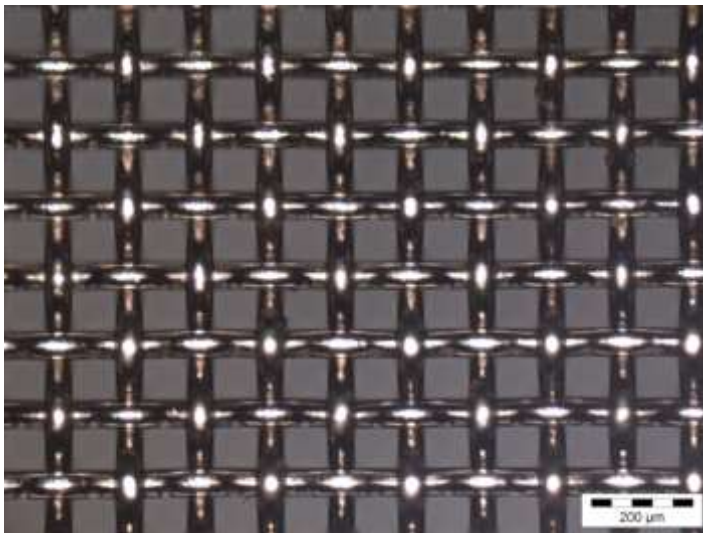
Figure 22 – Nickel mesh (light microscope)
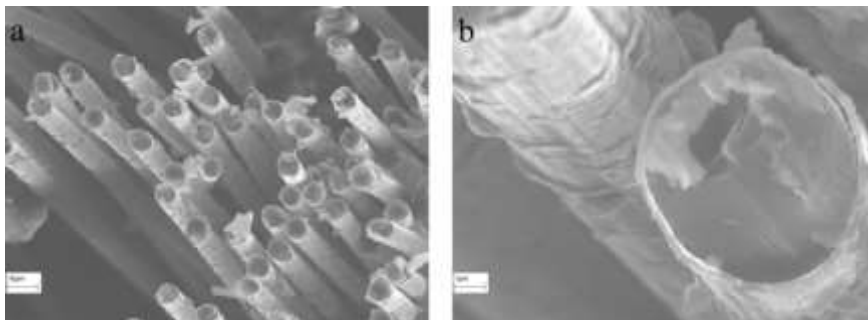
Figure 23 – Nickel coated carbon fibers (SEM, SE)

3.2   Sample manufacturing

3.2.1   Samples without fibers

3.2.1.1   Cold rolling

Using a roll trimmer 507 (Novus Dahle GmbH & Co. KG, Fig. 37) both foil and mesh were cut into stripes of two sizes, namely 30 mm-wide x 150 mm-long and 30 mm-wide x 145 mm-long, as the examples in Fig. 38, which were subsequently stacked up in a interlayered set up. The stacking consisted of 15 aluminium foil stripes interlayered with 14 nickel mesh stripes, comprising a thickness of approximately 2,4 mm, being 5 shorter aluminium and 4 shorter nickel stripes placed in the center of the stacking, easing the grip of the stacks by forging rolls and, thus, the cold rolling of the samples. Samples were cold rolled using a goldsmiths rolling machine (W40B, DIMA Maschinen-Handelsgesellschaft mbH, Fig. 39), aiming the production of massive samples.

Figure 24 – Roll trimmer 507 [41]

Figure 25 – Nickel mesh a) 150 mm-long b) 145 mm-long and aluminium foil
c) 145 mm-long and d) 150 mm-long stripes

Figure 26 – W40B goldsmiths rolling machine

After cold rolling, different heat treatments were tested, aiming to induce microstructural reorganization and phases composition change, intending to reduce deffects in size and number and provide higher mechanical properties to the material. The heat treatments were performed using an annealing furnace (N 41/H, Nabertherm GmbH, Germany, Fig. 40).

Figure 27 – N 41/H annealing furnace used to perform heat diffusion, solution and precipitation hardening heat treatments [42]

3.2.1.2 Diffusion annealing

Three different heat treatment cycles of diffusion annealing were tested, targeting diffusion of aluminium atoms into nickel, densificating the material and forming intermetallic phases. Heat treatment cycles consisted of heating the furnace up to 600°C and, after temperature stabilized, then placing the sample in the furnace for a determined dwell time (1, 3 or 5 hours) and letting the sample cool down inside the furnace. Fig. 41 shows temperature as a function of time for the experimented cycles of diffusion annealing.
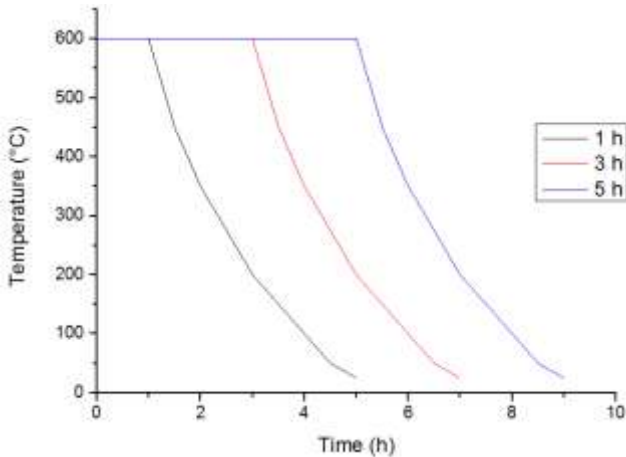
Figure 28 – Tested cycles of diffusion annealing of cold rolled samples (legend indicates dwelling time)

3.2.1.3 Solution annealing

A solution heat treatment was tested at 1300°C for 4 hours to assure that aluminium atoms would be solubilized in nickel. Samples were heated up in the furnace up to the dwelling temperature, which was held for 4 hours, then cooled down in the furnace, as describes Fig. 42.
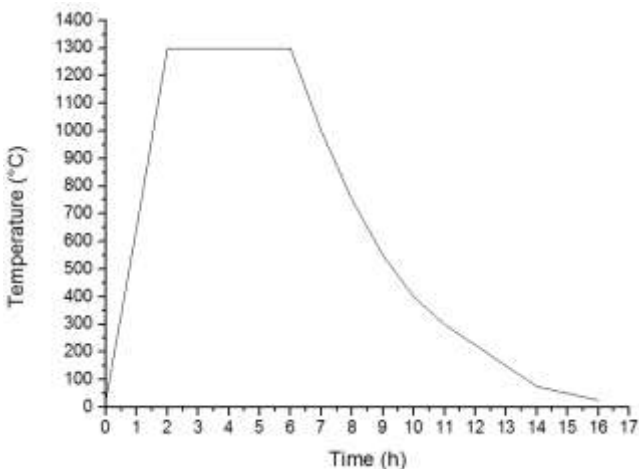
Figure 29 – Cycle of solution annealing of cold rolled samples

3.2.1.4 Immersion in aluminium melt

An alternative to fill the eventually remaining porosity was immersing samples in molten aluminium, that would also diffuse into nickel and drive the formation of nickel and aluminium compounds, which have higher mechanical and temperature resistance than aluminium and nickel not combined. The aluminum alloy 5754 (Al + 3wt% Mg) and comercially pure aluminum (99,5wt%) were melted in a melting furnace (K 2/10, Nabertherm GmbH, Germany, Fig. 43). The melt was at 900°C, samples were initially at room temperature and were held for 15 s in the melt.

Figure 30 – Melting furnace Nabertherm K 2/10 [42]

3.2.1.5 Precipitation hardening

After the immersion in the aluminium melt some samples went through a precipitation hardening heat treatment, with the purpose of improving material's strength and temperature resistance. Samples were heated up to 1300°C, temperature which was held for 4 hours, then cooled down to 1080°C and remained at this temperature for 2 hours, finally cooling down to room temperature (Fig. 44). This treatment was

designed based on the heat treatment performed on nickel super alloys for turbine blades[43].
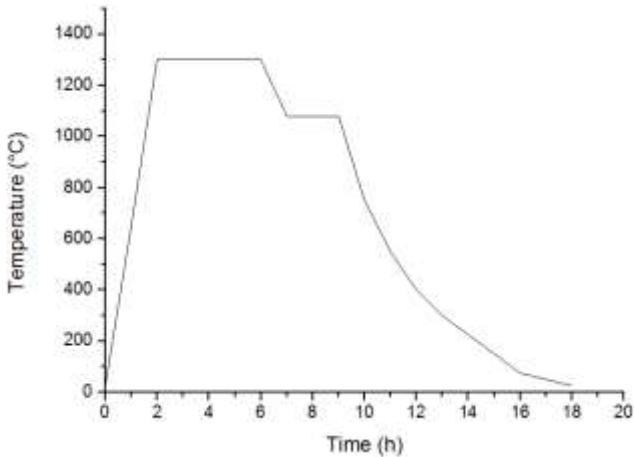
Figure 31 – Cycle of precipitation hardening of cold rolled and immersed samples

Finally, the manufacturing route for the samples without fibers was defined as it follows in Fig. 45:

- Interlayered stacking of aluminium foil and nickel meh stripes;
- Cold rolling of the stacks with an approximate 70% thickness reduction;
- Vertical immersion of the sample in aluminium melt;
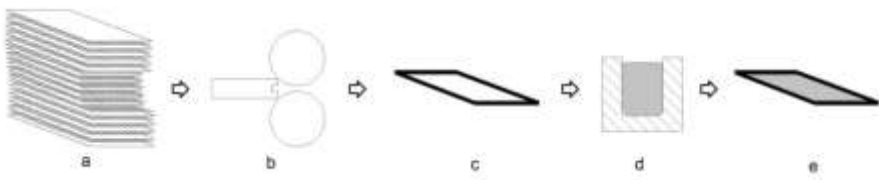
Figure 32 – Manufacturing of samples without fibers: a) interlayering aluminium foils and nickel mesh stripes b) cold rolling c) cold rolled sample d) immersion in aluminium melt e) final sample

3.2.2   Samples with fibers

Samples with fibers were prepared through hand lay-up of aluminium foils, nickel mesh stripes and nickel coated carbon fibers, in a set-up that interlayered aluminium foils and nickel mesh or carbon fibers aligned along samples length, alternating the latest two between aluminium foils. Components were maintained together by an aluminium adhesive tape (1170, 3M, USA), since cold rolling would destroy the carbon fibers, so they could still be immersed in melt. These samples were produced using 22 aluminium foil stripes, 8 nickel mesh stripes and 7 layers of unidirectionally aligned carbon fibers, held together with aluminium adhesive tape and then vertically immersed in aluminium melt at 900°C for 15 s, processing summarized in Fig. 46.
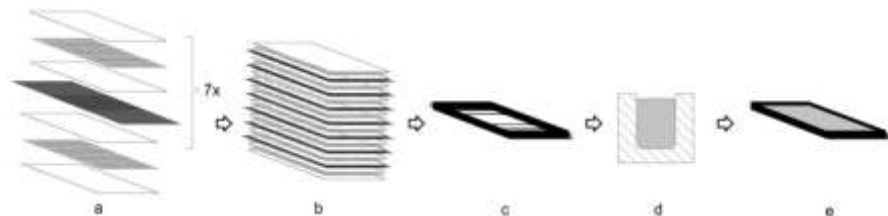
Figure 33 – Manufacturing of samples with fibers: a) hand lay-up of aluminium foils, nickel mesh and carbon fibers b) stacked layers c) layers held together with aluminium tape d) immersion in aluminium melt e) final sample

3.3   Characterization

3.3.1   Metallographic preparation

Samples were cold embedded to avoid eventual microstructure changes due to temperature, ground with silicon carbide grinding papers 500, 1200, 2400 and 4000 mesh by a RotoForce-4 grinding machine (Struers A/S, Denmark) and then polished by a Tegramin-25 Polishing machine (Struers A/S, Denmark) using 3 μm and 1 μm polishing suspensions.

3.3.2   Light microscopy

Microstructural analyses were firstly conducted using a DM LM light microscope (Leica Microsystems GmbH, Germany), with light

field microscopy, willing to assure the continuity of the samples microstructure.

3.3.3 Scanning electron microscopy

Scanning electron microscopy techniques of secondary and back-scattered electrons detection were conducted with a LEO 1430 electron microscope (Carl Zeiss AG, Germany), to gather more detailed information about the phases resulting from the manufacturing process, as well as from the fracture surfaces resulting from the bending tests.

3.3.4 Energy-dispersive X-ray spectroscopy

In order to qualitatively profile the composition of the formed phases, energy-dispersive X-ray spectroscopy (EDX) was used in line scan and punctual analysis, a tool provided by the LEO 1430 electron microscope and by the Hitachi Tabletop Microscope TM3030 (Hitachi High-Technologies Corporation, Japan), aiming to evaluate the effects of aluminium infiltration into the samples.

3.3.5 X-ray diffractography

Identification of the final material's crystalline phases was performed via X-ray diffractography (XRD), with an Emperial diffractrometer (PANalytical B.V., Netherlands), using cobalt Kα radiation (CoKα), 40 kV electric tension and steps varying from 0,03 °/s to 0,3 °/s.

3.3.6 Microhardness test

Metallographic samples were used to measure microhardness of the present phases with a microhardness testing machine (VMHT30M, Leica Microsystems GmbH, Germany). Vickers microhardness was measured using 0.01 kgf of load.

3.3.7 Tensile tests

Tensile and bending tests were performed using a universal testing machine Z010 (Zwick GmbH & Co. KG, Germany), both with 10 mm/min loading rate until rupture. Tensile test samples were machined using an anglegrinder and given the dimensions represented in

Fig. 47 below, based on GUNT WP 600 Creep Testing Machine –
Experiment Instruction ([44]).
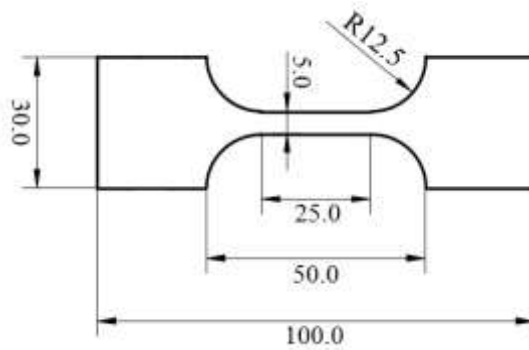
Figure 34 – Representation of tensile test sample (dimensions in mm)

3.3.8 Bending tests

Based on the norm DIN EN 658-3:2002 ([45]), bending samples
were cut using a tile saw into the dimensions 10 mm x 80 mm, leaving
thickness unchanged. Flexural strength was calculated following the
equation

$$\sigma = \frac{3F(L - L_i)}{2bh^2} \tag{2}$$

in the norm, where σ is the flexural strength, in MPa, F is the load that
caused the failure of the sample, in N, L the length of the sample, in
mm, L_i, the distance between the supporting rollers, in mm, b the width
of the samples, in mm, and h the thickness of the sample, in mm as well.
The elastic modulus was calculated using the equation[46]

$$E = \frac{\Delta P}{\Delta \delta} \frac{(3L_s L^2 - 4L_s^2)}{48I} \tag{3}$$

where E is the elastic modulus, in MPa, $\frac{\Delta P}{\Delta \delta}$ is the slope of linear
portion of the curve load x deflection, in N/mm, L_s is the distance

between the supporting rollers, in mm, L is the length of the sample, in mm and I the moment of inertia of the sample, in mm^4, given by

$$I = \frac{bh^3}{12} \tag{4}$$

An example of the setup of the 4-point bending tests is shown in Fig. 48.
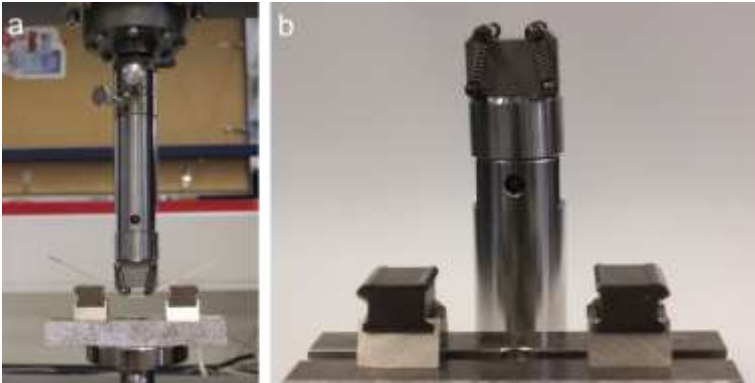
Figure 35 – Setup of the bending test a) example of test b) detail of the supporting and loading pins

3.3.9 Fiber content analysis

The fiber content in the samples was measured with the softare Imago[46], an image analysis tool for microstructural characterization, using picutres made with the SEM and light microscope, to estimate the local volume fraction of incorporated fibers in the samples by binarizing the pictures in black and white and then measuring the areas occupied by each color.

4   RESULTS AND DISCUSSION

4.1   Samples without fibers

4.1.1   Sample manufacturing

4.1.1.1 Cold rolling

The result of the cold rolling step were flat samples with smooth surface (Fig. 49). Stacks were around 2,4 mm thick and cold rolled samples approximately 0,7 mm, being the thickness reduction close to 70%, found to be high enough to bind foils and mesh mechanichally, though still low enough to deliver flat samples and not to damage the layers.

Figure 36 – Rolled sample

Light microscopy showed that mechanical work by itself did not suffice to fill the empty spaces of the nickel mesh and produce massive samples, resulting in remaining porosity. The result of the cold rolling step can be seen in Fig. 50, which shows the cross section of the mesh, here seen as smooth white circles, and the aluminium layers, the rough matrix envolving the circles, in some points even welded together through plastic deformation.
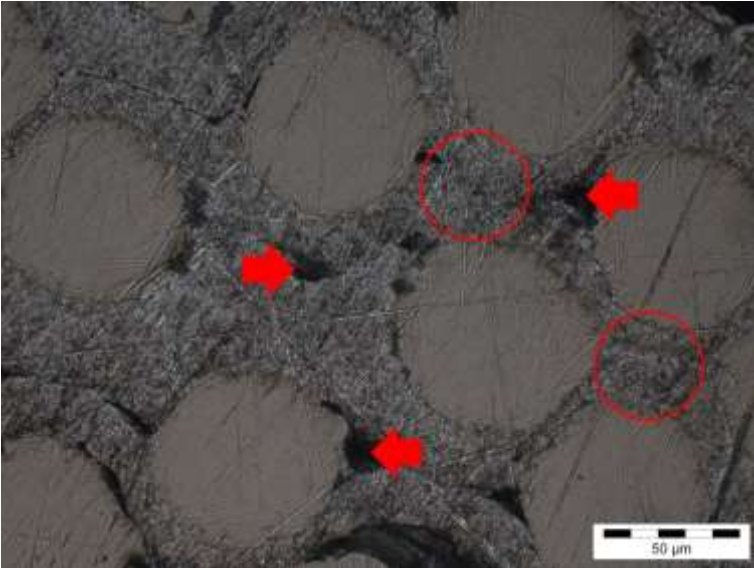
Figure 37 – Cross section of rolled sample showing voids (arrows) and welded foils (circles) (light microscope)

In order to provide the material with high mechanical properties, different sets of heat treatment were tried, aiming to form nickel-aluminum intermetallic phases, whose results are shown in the following sections.

4.1.1.2 Diffusion Annealing

The results of the three diffusion heat treatment cycles are shown in Fig. 51, Fig. 52 and Fig. 53 with 1 h, 3 h and 5 h dwell time at 600°C, respectively. The diffusion annealing cycle with 1 h-dwelling time promoted the diffusion of aluminium for not more than 5 μm into nickel, pointed out by the arrows in Fig. 51, causing not much change in microstrucutre. The 3 h-dwelling time cycle showed many sites of intermetallic phase nucleation (showed by the arrows in Fig. 52), but deffects were not removed (circles in Fig. 52). After annealing for 5 hours at 600°C, some more intermetallic phase was present, but also voids coarsened, probably due to volume shrinking caused by the formation of a more dense phase than aluminium. Therefore, diffusion annealing was found to be inappropriate for the production of massive samples, so other approaches were tried.
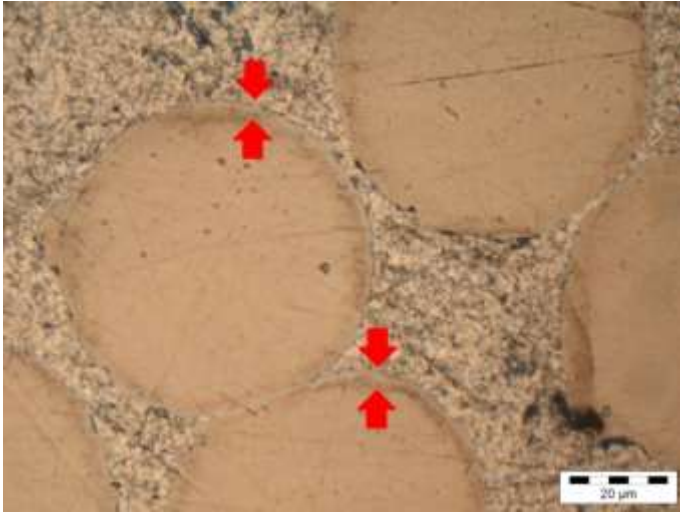
Figure 38 – Rolled sample after diffusion annealing for 1 hour at 600°C.
Arrows show diffusion of aluminum into nickel (light microscope)
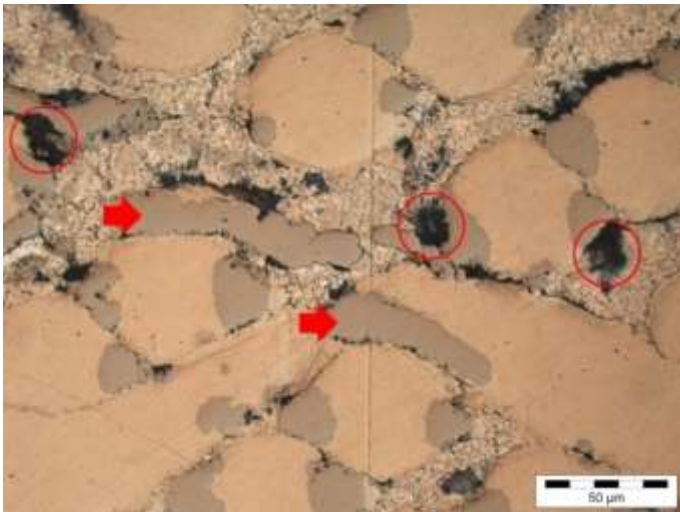
Figure 39 – Rolled sample after diffusion annealing for 3 hours at 600°C.
Arrows show intermetallic precipitates and circles show voids (light
microscope)
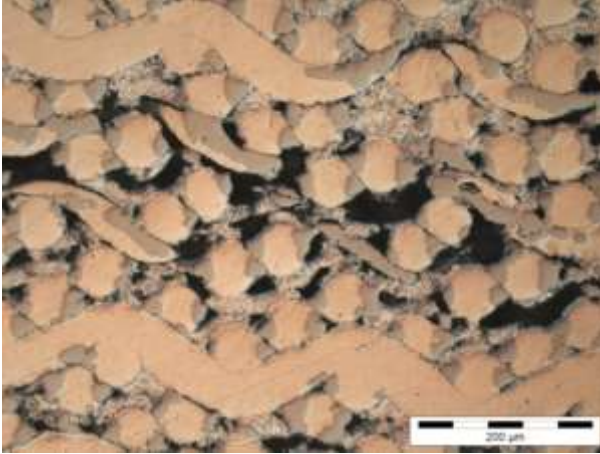
Figure 40 – Rolled sample after diffusion annealing for 5 hours at 600°C (light microscope)

4.1.1.3 Solution Annealing

Although all the aluminium present in cold rolled samples was completely solubilized by nickel after 4 h at 1300°C, the heat treatment was still not effective on producing a void-free sample. Fig. 54 shows that aluminium and nickel combined with each other in a polycristalline phase, leaving coarsened pores.
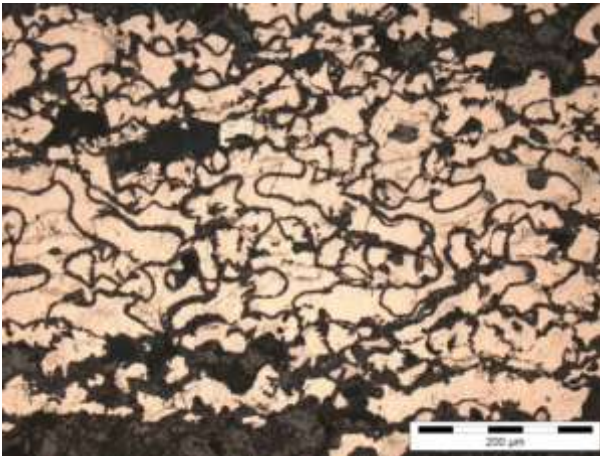
Figure 41 – Rolled sample after solution annealing for 4 hours at 1300°C (light microscope)

4.1.1.4 Immersion in aluminium melt

Samples had their surface turned rougher after the immersion in melt, when compared to the surface roughness after cold rolling. Some melt slag adhered to the samples surface, forming irregularities, as shown in Fig. 55. Porosity almost vanished with the immersion of the samples in aluminium melt, because it filled the empty spaces, leaving practically no voids, as shown in Fig. 56. Not only that, the high temperature of the melt promoted the diffusion of aluminium into nickel, as well as of nickel into the aluminium melt, initiating simultaneously the formation of several intermetallic phases at the surface of the nickel mesh. After the 15 s in the melt at 900°C, the material was found to be composed by four phases, which are shown in more detail in Fig. 57.

Figure 42 – Cold rolled sample after immersion in aluminium melt at 900°C for 15 s
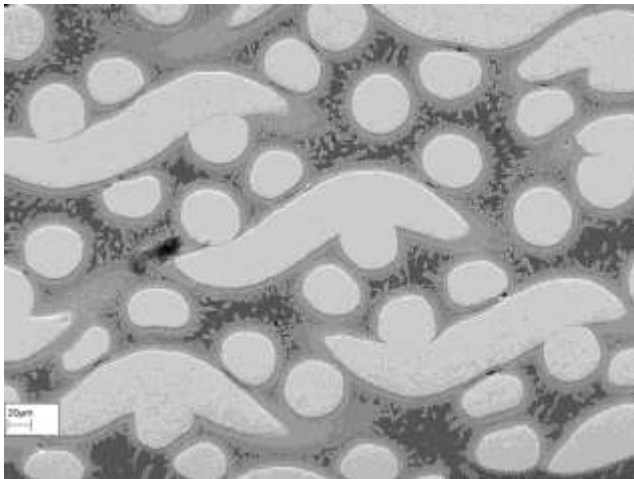
Figure 43 – Rolled sample immersed in aluminium melt at 900°C for 15 s (SEM, SE)
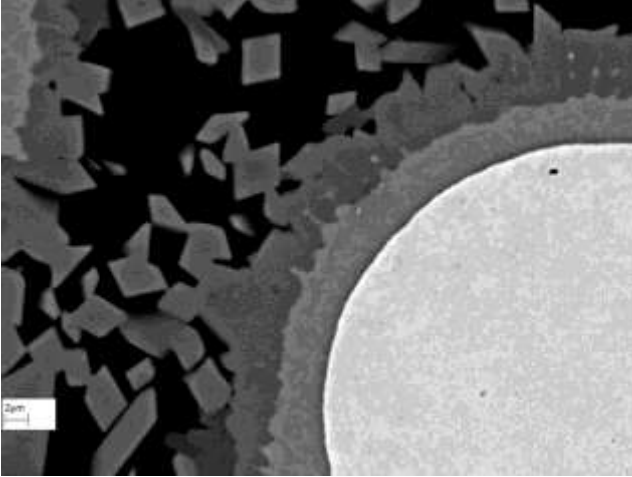
Figure 44 – Rolled sample immersed in aluminium melt at 900°C for 15 s
(SEM, SE)

4.1.1.5 Precipitation heat treatment

Precipitation hardening experiments were conducted with samples that were immersed in aluminium melt, intending to solubilize all the aluminium in nickel and form precipitates that would work as a strengthening mechanism. The solubilization of aluminium atoms in nickel and the volume shrinkage due to the precipitation of a denser phase resulted in voids around the mesh structure (Fig. 58). As such a high porosity would weaken the material too much, the precipitation hardening was not considered an useful manufacturing step in the present work.
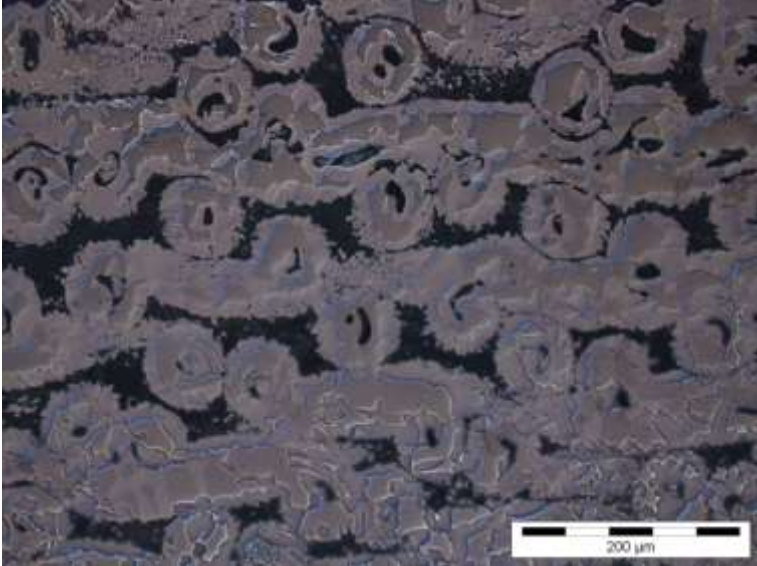
Figure 45 – Rolled sample immersed in aluminium melt at 900°C for 15 s, then submitted to precipitation heat treatment (light microscope)

The final manufacturing route for samples without reinforcement, as described in section 2.2.1 in Fig. 45, consists in:

- Interlayered stacking of aluminium foil and nickel mesh stripes;
- Cold rolling of the stacks with an approximate 70% thickness reduction;
- Immersion in aluminium melt at 900°C for 15 s;

4.1.2 Characterization

4.1.2.1 Scanning electron microscopy

Predominantly, four crystalline phases comprised the microstructure of the samples produced without fiber reinforcement, which are in Fig. 59. The black matrix (a), an outter dark gray layer (b), an inner gray layer (c) and light gray structures (d).
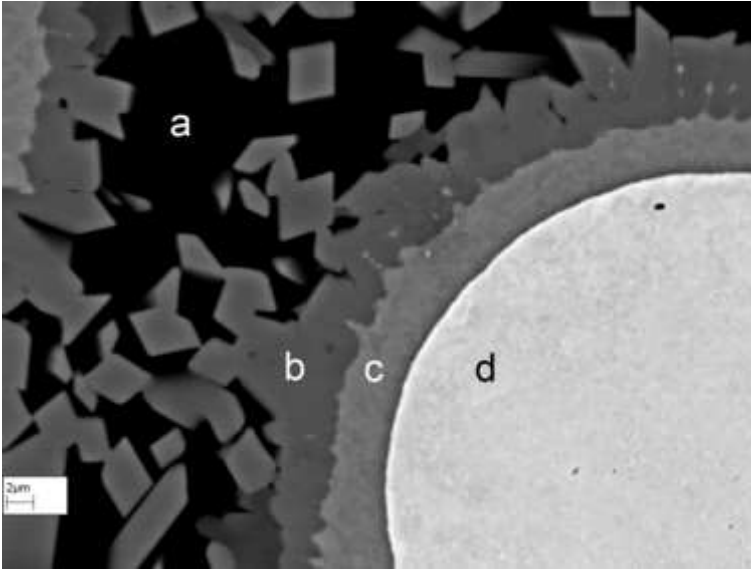
Figure 46 – Microstructure of the samples without reinforcement showing predominantly four different phases (SEM, BSE)

The phenomenon of simultaneous growth of multiple layers as a result of diffusion reaction in binary systems has been observed and studied for decades, with much attention to the nickel-aluminum system. Hickl and Heckel ([48]) analyzed the diffusion reaction of pure aluminum and pure nickel at 870°C, 930°C and 1000°C for 15 minutes to 4 hours, as well as the growth or consumption of phases after a further treatment at 1000°C. They also modelled the kinetics of the phenomenon at the given temperature range, finding out that it follows the steps:

- the first phase to be formed is Ni_2Al_3, whose growth parabolic decreases with time
- following phases are NiAl, Ni_3Al and Al solubilized in Ni, according to the phases presented in the Ni-Al diagram (Fig. 60) along the increasing Ni content
- the layer growth is major controlled by the initial concentration of Al and Ni and the concentration of intermetallics at the interphases of the layers
- during the homogenization treatment at 1000°C, the NiAl phase grew, completely consuming the Ni_2Al_3 layer

As the parameters used by Hickl and Heckel are similar to the ones of this work, one could expect the reaction between nickel mesh and aluminum melt of the colled rolled samples to present a similar behavior. Voudouris et. al ([49]) observed the formation of intermetallic multilayers in the CVD coating of nickel at 1000°C as well, using FeAl (52at% Al) as Al source, the formation of Ni_2Al_3 was not reported though (as it should, observing Fig. 60), probably because its amount formed was little and then consumed by the NiAl during the heat treatment, similar to the results obtained by Wierzba, et al ([50]). Beyond that, Rizov and Magdeski ([51]) reported the dependence of the Ni_2Al_3 layer thickness on the nickel content of the aluminum melt.
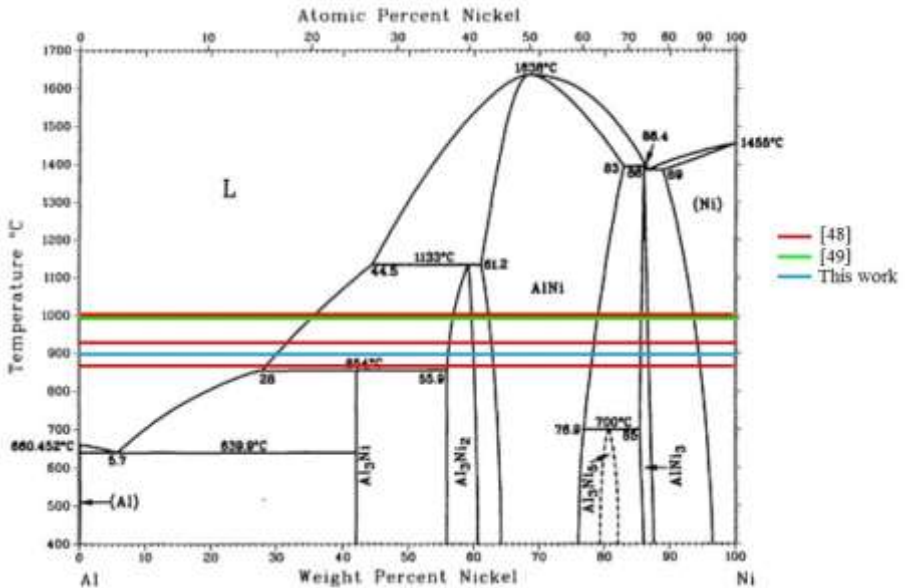
Figure 47 – Ni-Al phase diagram showing the temperatures used in references [48], [49] and the present work

Since the samples were cold rolled and aluminum foils were very thin (approx. 13 μm), nickel mesh were plastically deformed and very close to each other, so that the growth of intermetallic phases towards each other at the interface of nickel mesh layers resulted in the formation of cracks and voids (Fig. 61).

Fig. 62 a shows in more detail a filling deffect, probably caused either by incomplete infiltration of the structure or pore formation due to

quick diffusion into the other phases formed, meanwhile Fig. 62 b shows cracking at the interface of two growing portions of the same phase, which consumed the aluminum melt, but might not have had time at the processing temperature to coarsen, leaving deffects between them.
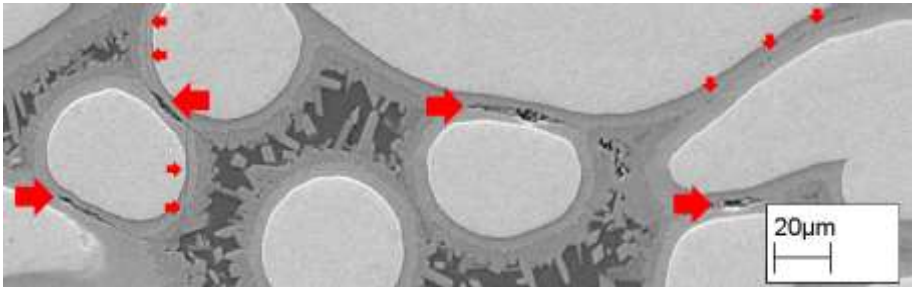
Figure 48 – Cracks and voids resulted from the concurrent growth of intermetallic phases (SEM, SE)
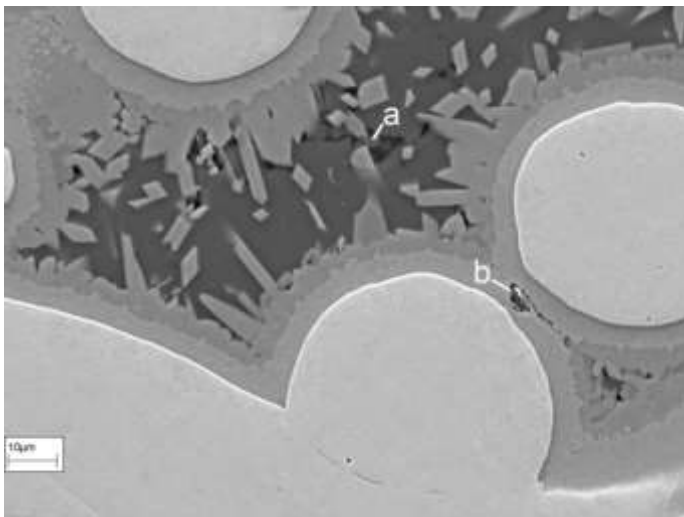
Figure 49 – Microstructure of the samples without reinforcement a) and b) showing deffects of infiltration (SEM, SE)

The fracture surface of the samples after the bending test is depicted in Fig. 63, exhibiting a very irregular surface, showing nickel mesh wires that underwent through necking and rupture, and holes, from which other nickel wires were teared off. The necking of the nickel

mesh wires might have acted as a pull out mechanism providing the sample with some ductility and toughness.

Grains were found to be fairly equiaxed and fine, as shown in Fig. 64, which also presents microcracking around the pulled-out nickel wire, another mechanism that contributes to stresses redistribution and, consequently, toughening. However, fracture showed an intergranular character, what characterizes an elevated brittleness. Some particles can also be identified in the picture, here appearing white, which are probably intermetallic compounds.
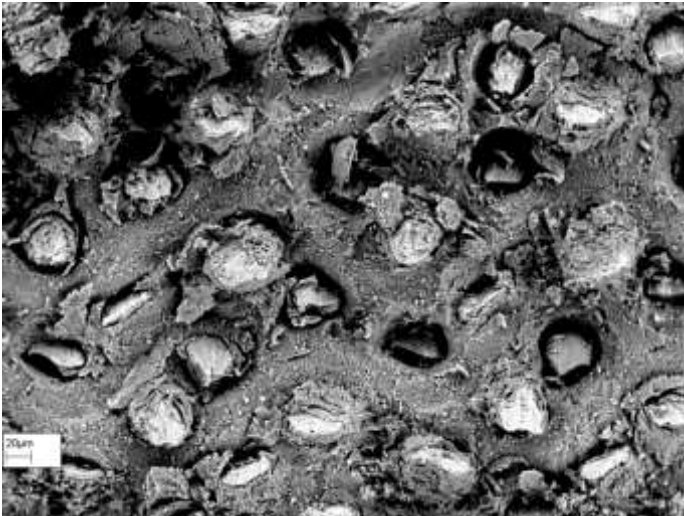
Figure 50 – Fracture surface of a sample without reinforcement after the 4-point bending test (SEM, BSE)
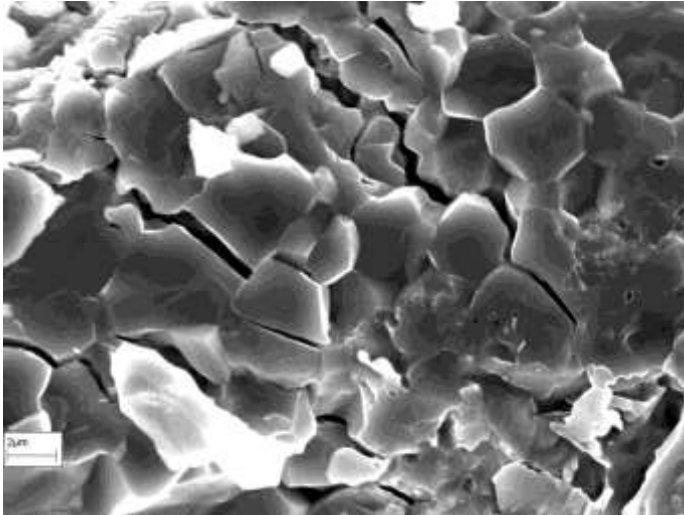
Figure 51 – Microcracking in the surroundings of a wire of nickel mesh (SEM, BSE)

4.1.2.2 Energy-dispersive X-ray spectroscopy

A cold rolled sample, which was immersed in aluminum melt, was analyzed over the yellow line showed in Fig. 65, the result shown in Fig. 66. The light gray circle (Fig. 66 d) is might still be pure nickel from the nickel mesh, until its surface, where reactions with the aluminum melt formed two intermetallic compounds (Fig. 66 b and c), whose composition cannot be distinguished only with the EDX analysis. The matrix (Fig. 66 a) has a high aluminum content, but might not be pure aluminum. The presence of magnesium was of little importance, as it is very likely to be solubilized in aluminium and/or nickel and can easily be mistaken for aluminum in this analysis.

For an estimation of the composition of the different phases, EDX measurements were also carried out punctually. Fig. 67 shows the spots analyzed in a sample without fibers, whose corresponding results are shown in Table 8. According to the results spot 1 (Fig. 67) is very likely to be pure nickel, meanwhile spot 2 could be NiAl or even Ni_2Al_3 and spot 3 could be Ni_3Al. According to the Ni-Al phase diagram, spot 4 could be $Al + NiAl_3$. It should be noticed that the accuracy of EDX is not appropriate to measure the exact composition of the phases, so that these results roughly reflect the reality.
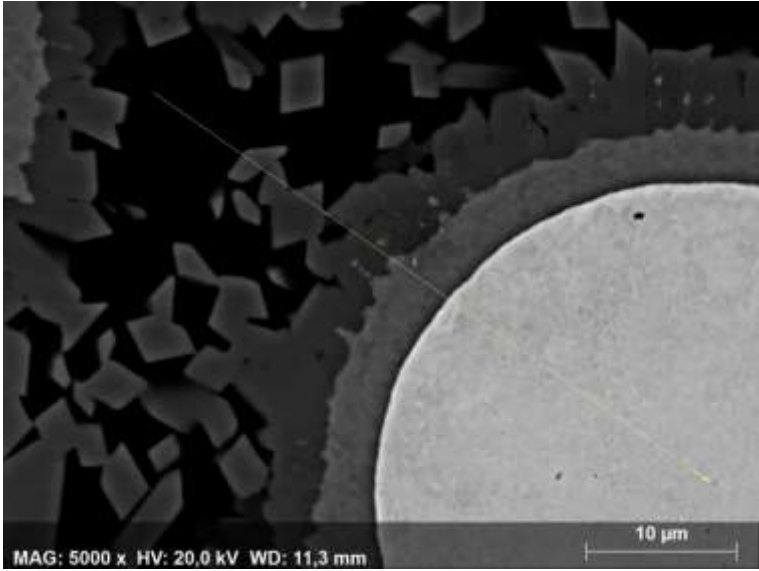
Figure 52 – Line over the cold rolled sample which was scanned with EDS (SEM, BSE)
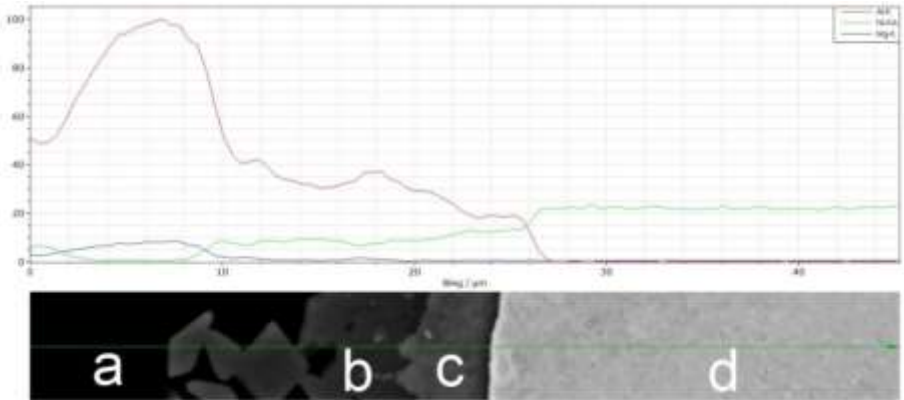
Figure 53 – Profile of elements over the EDX scanning of a cold rolled sample
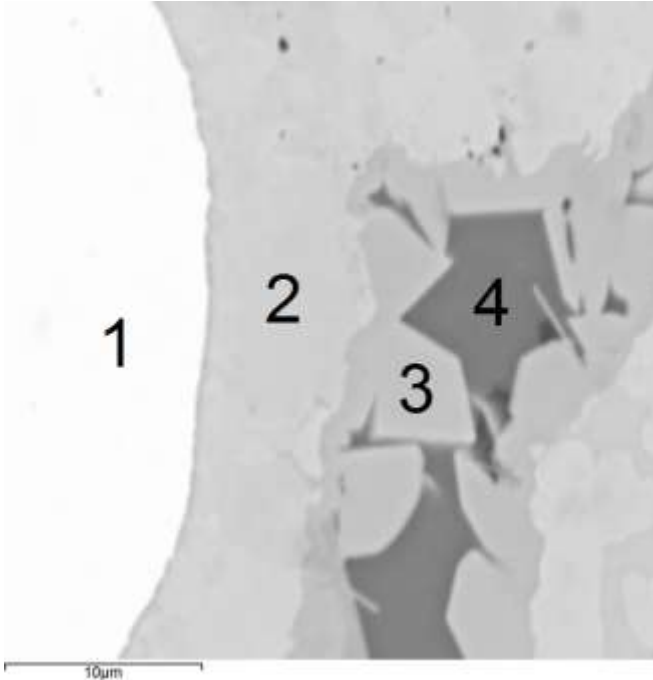
Figure 54 – EDX spot analysis of a sample without fibers

Table 8 – Results of the EDX spot analysis of the sample without fibers

Spot	Al (at%)	Ni (at%)	Mg (at%)
1	3	97	-
2	54	45	-
3	20	78	2
4	80	12	6

4.1.2.3 X-ray diffractography

Crystalline phases found in the X-ray diffractography of cold rolled samples immersed in pure aluminum melt (Fig. 68) agree with phases found in the literature (Ni_2Al_3, NiAl, Ni)[47,48] and with the EDX results. The presence of Ni_3Al_4, which is absent in the Ni-Al phase diagram, was also suggested as a possibility, but always sharing peeks with stable phases, more likely to be found.
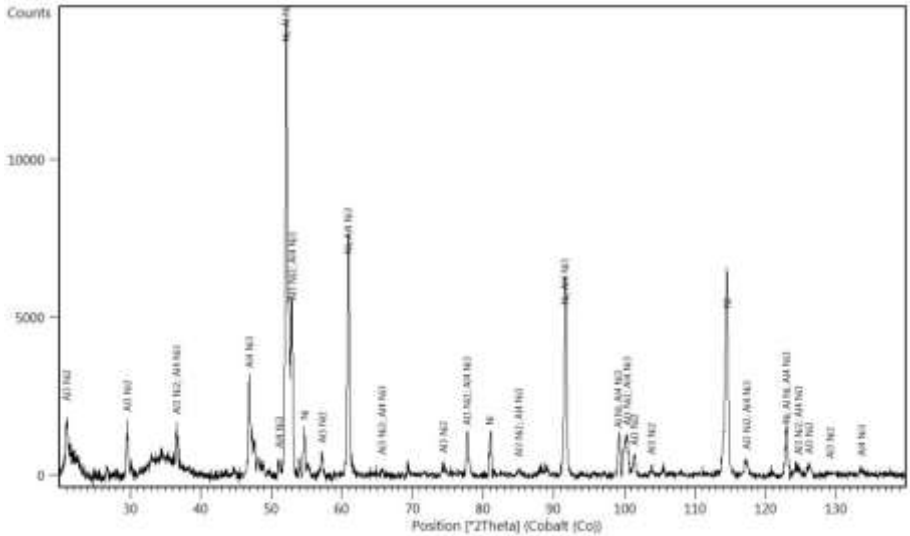
Figure 55 – X-ray diffractography of a cold rolled sample after immersion in
pure aluminum at 900°C for 15 s

Even though the solubilization heat treatment was not integrated
in the manufacturing process of the samples, the crystalline phases
formed by it were also investigated (Fig. 69), aiming to check its
effectiveness and the microstructure evolution at high temperatures. It
was found out that the solubilization did not fully take place, as two
phases were present after the heat treatment, $Ni_{0,9}Al_{1,1}$ and Ni_3Al,
similar to the literature[47-49]. Oxidation also occured during the
solubilization, forming Al_2O_3.
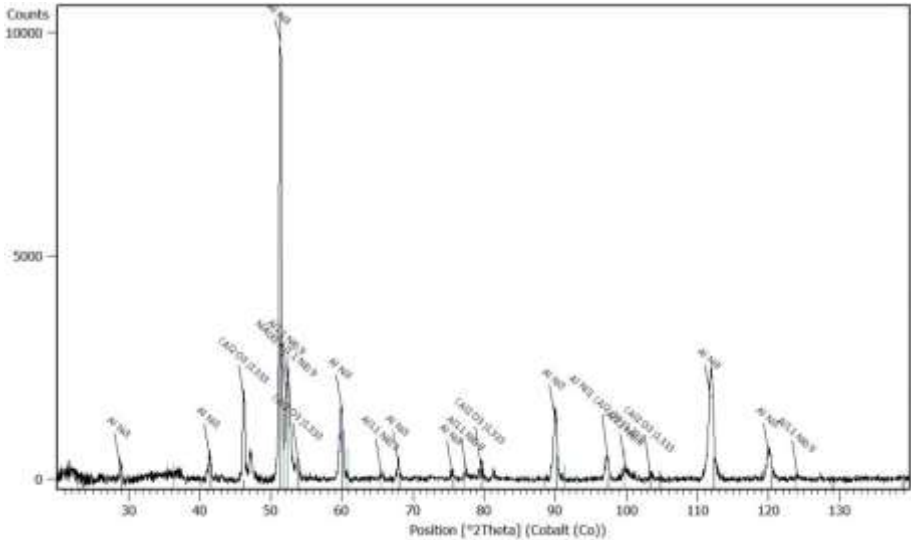
Figure 56 – X-ray diffractography of a cold rolled sample after immersion in
pure aluminum and submitted to solubilization heat treatment

4.1.2.4 Microhardness test

The Vickers microhardness of the phases present in the
microstructure of cold rolled samples was measured using a 0.01 kgf
load. Data is set in Table 9 and indentations are shown in Fig. 70.

Table 9 – Vickers microhardness of phases formed during the immersion in
aluminium melt (letters refer to Fig. 70)

Phase	Nickel (a)	Dark gray (b)	Outter gray (c)	Matrix (d)
Vickers Microhardness (HV)	174	944	439	176
	161	970	431	185
	166	998	474	192
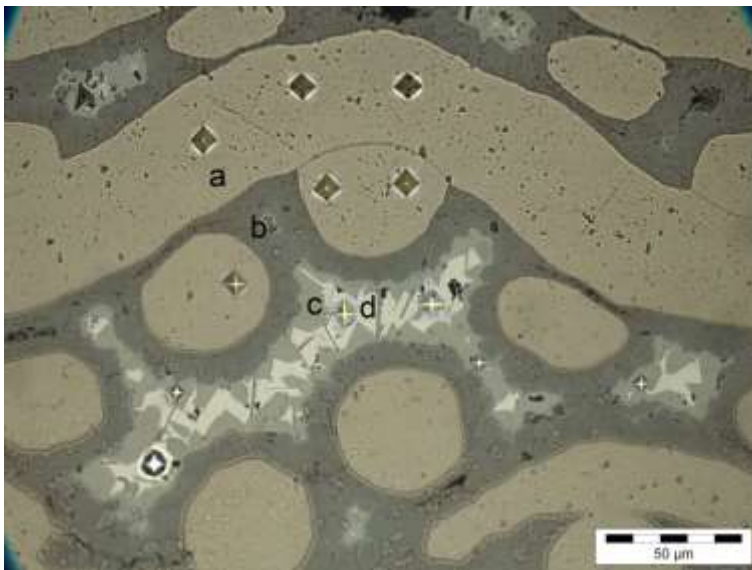
Figure 57 – Microhardness measurements of a sample without fiber
reinforcement (light microscope)

The measured hardness for the inner gray phase (Fig. 70 b) are
comparable to that of Ni_2Al_3 produced by high-pressure hot pressing (5
GPa at 1000°C) consolidation (approximately 970 HV) by Krasnowski,
et al ([52]), measured with 0.2 kgf though, meanwhile the values
obtained for the light gray phase (Fig. 70 c) correspond to the values
obtained for non stoichometric NiAl (between 400 and 500 HV), by
Westbrook ([53]). Hardness of nickel (Fig. 70 a) is in the commercially
acceptable range, i.e. between 80 and 300 HV[54]. As no comparable
hardness values for the matrix (Fig. 70 d) were found in the Ni-Al
system, besides nickel, it may be a nickel-rich phase, containing
aluminum as substitional solute, corresponding to the studies for the
given parameters[48,50].

4.1.2.5 Tensile test

A single sample without fibers was tested under tensile.
Because of the brittleness of the material, other samples were tested
under bending. The sample presented elastic modulus of 38 GPa, yield
strength of 25 MPa, ultimate tensile strength of 50 MPa and elongation
of 1%. Fig. 71 shows the tensile test curve of the sample without fiber.

The result for the sample reinforced with fibers is plotted with a dashed line, for comparison.
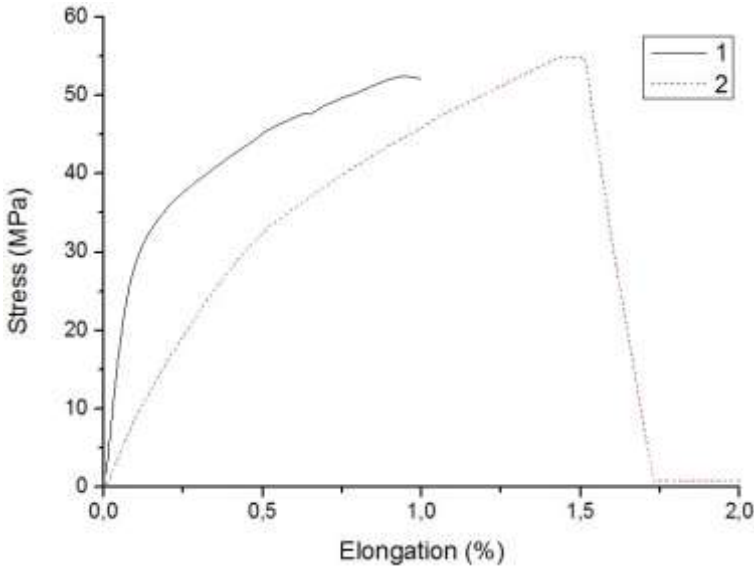
Figure 58 – Tensile test curve for 1 - sample without fibers 2 - sample with fibers

4.1.2.6 4-Point bending test

As samples exhibited a brittle behaviour, they were tested under bending, so that the data could be properly treated. Non-reinforced samples presented similar responses, usually describing an elastic response step, followed by plastic deformation with increasing stress, plastic deformation with decrasing stress and finally abrupt rupture (Fig. 72). The plastic deformation is likely to be attributed to the necking of nickel wires. The results of the bending tests are in Table 10. Weibull statistics was used to assess the characteristical strength and Weibull modulus for the set of cold rolled samples (Fig. 73), calculated as 210 MPa and 4.5, respectively. As the intermetallic phases present in the samples are fragile, a fragile behavior was expected, however, the absolute values are considerably low, property owed to the high density of cracks in the microstructure, formed during concurrent growth of hard phases. Also, as samples were thin and could not be submitted surface machining, the roughness resulting from the processing probably

played an importat role on the low measured strength values and scattering of the data, by initiating cracks on the surface of the samples.
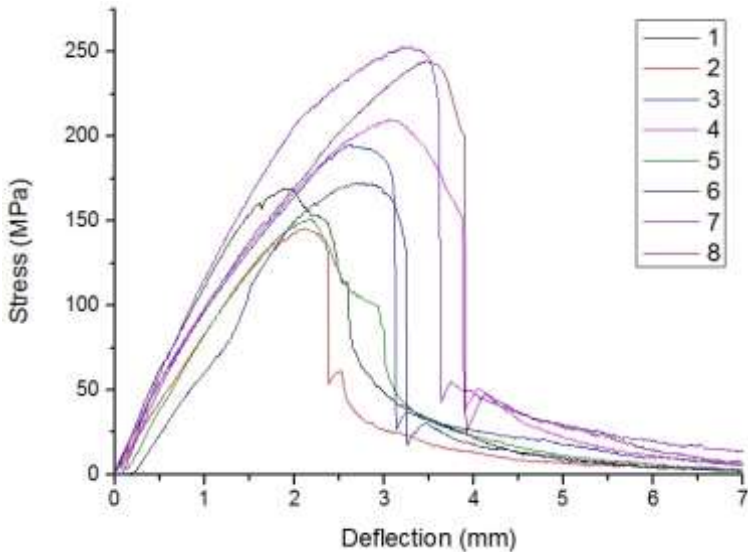
Figure 59 – Bending tests curves for samples without reinforcement

Table 10 – Bending tests results of samples without reinforcement

Sample	Thickness (mm)	Bending Strength (MPa)	Elastic Modulus (GPa)
1	0.7	169	111
2	0.8	146	74
3	0.8	195	71
4	0.8	210	66
5	0.8	151	70
6	0.8	172	65
7	0.7	253	84
8	0.7	244	79
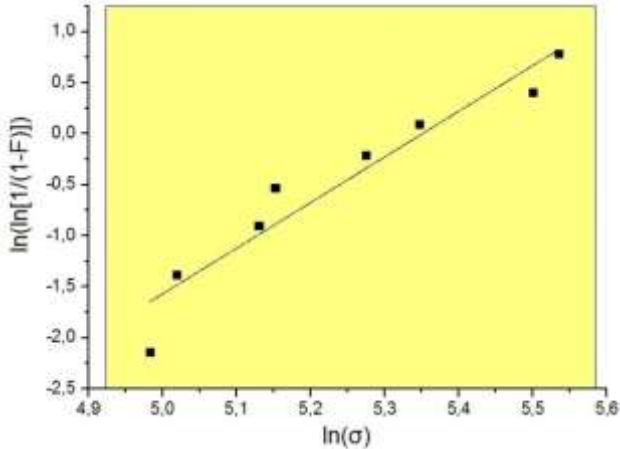
Figure 60 – Weibull plot of the bending tests of samples without reinforcement

4.2   Samples with fibers

4.2.1 Sample manufacturing

Since the manufacturing process for the multiphase intermetallic material had been defined, it was used as a matrix for the production of a carbon-fiber reinforced composite, but instead of cold rolling the samples, they were held together by an aluminium adhesive tape, so that they could be immersed in the melt and then become a massive sample. Carbon fibers were incorporated to the material as depicted in section 2.2.2, Fig. 46. Example of samples before and after being immersed in aluminium melt is shown in Fig. 74 and 75, respectively.

Figure 61 – Sample with carbon fibers before immersion in aluminium melt

Figure 62 – Sample with carbon fibers after immersion in aluminium melt

In the longitudinal section (Fig. 76), it can be seen that the carbon fibers are not perfectly aligned, as they show different area of their length in the plane of the metallographic section. In that figure, pure nickel is only to be found close to the surface, meanwhile in the bulk of the sample all nickel is combined with aluminium in the form of intermetallics.

The cross section (Fig. 77) shows that carbon fibers were more concentrated in some regions of the sample, where consequently the aluminium melt could not infiltrate, thus where discontinuities are concentrated, what could be the reason for the nickel not to have reacted in some portions of the sample. The same picture also shows that intermetallic phases show fair anisotropy, since nickel wires were aligned with both cross and longitudinal sections and the prefered diffusion direction of nickel into aluminium was towards all perpendicular directions to those wires.
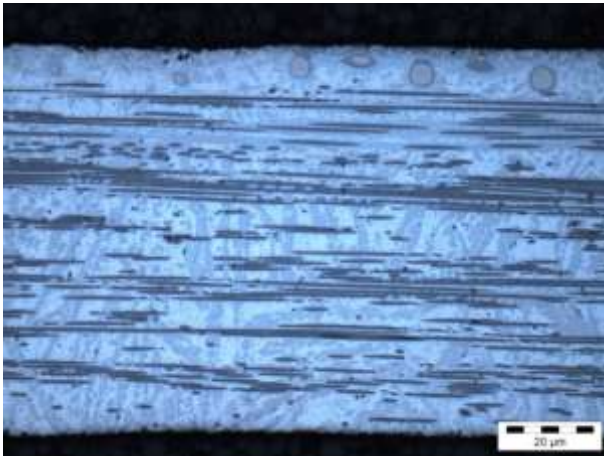
Figure 63 – Longitudinal section of a carbon-fiber-reinforced sample after immersion in aluminium melt at 900°C for 15 s (light microscope)
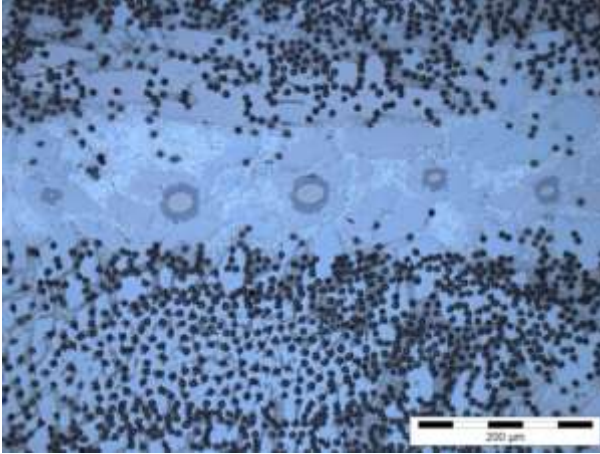
Figure 64 – Cross section of a carbon-fiber-reinforced sample after immersion
in aluminium melt at 900°C for 15 s (light microscope)

4.2.2   *Characterization*

4.2.2.1   Scanning electron microscopy

Intermetallic compounds were also formed in samples reinforced with carbon fibers, however, in a smaller amount, because of the lower content of nickel, and also with little orientation, perpendicular to the direction of the fibers (Fig. 78), not as homogeneous as in the cold rolled samples, probably due to nickel solubilization in aluminum followed by the formation of intermetallic phases during cooling. The nickel coating of the carbon fibers was solubilized in the aluminum melt, forming nickel intermetallic compounds adjacent to the fibers, but leaving their surface in direct contact with the matrix (Fig. 79). Bonding between reinforcement and matrix was apparently strong, with almost no presence of deffects.
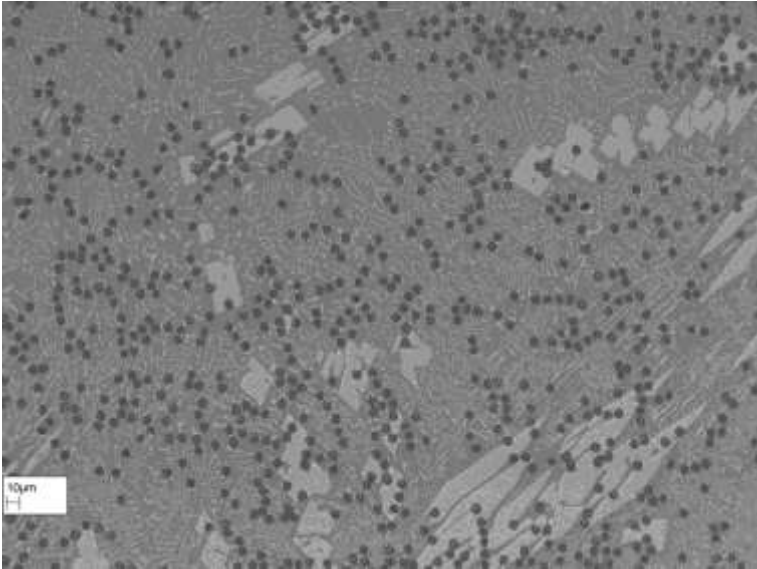
Figure 65 – Microstructure of reinforced samples (SEM, SE)
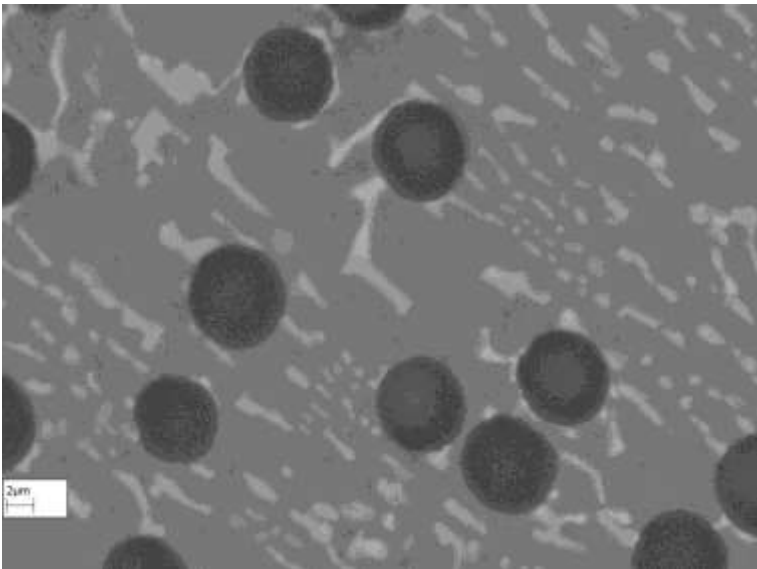
Figure 66 – Detail of the microstructure of reinforced samples (SEM, SE)

The fracture surface of the reinforced samples showed a brittle behavior (Fig. 80), not expected for fiber reinforced materials. No trace

of the typical toughening mechanisms provided by fibers, like crack bridging, pull out or crack deflection, was found in the microstructure and the surface of the fractured fibers also presented signs of brittle fracture (Fig. 81). This phenomenon can be the effect of the diffusion of aluminum into the fibers, forming aluminum carbides, which, by their turn, are also brittle, providing little contribution for the toughening of the matrix.

Fig. 82 shows more fibers that presented a very brittle fracture, but also a region with high concentration of fibers that, for this reason, could not be regularly infiltrated by the aluminum melt and become massive. This results in voids and deffects that weaken the material.
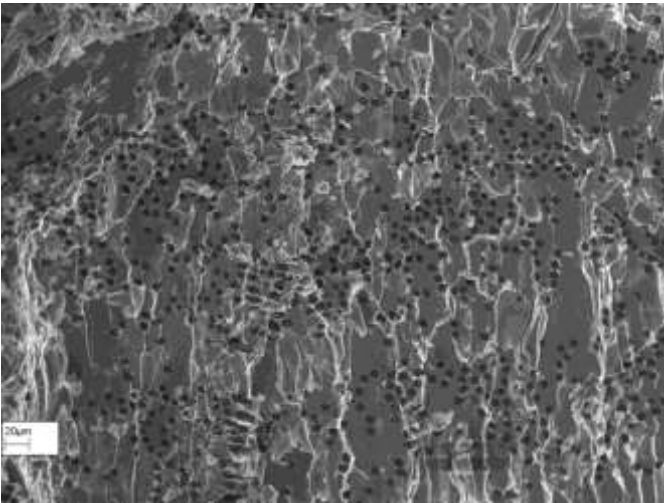
Figure 67 – Fracture surface of the reinforced samples (SEM, SE)
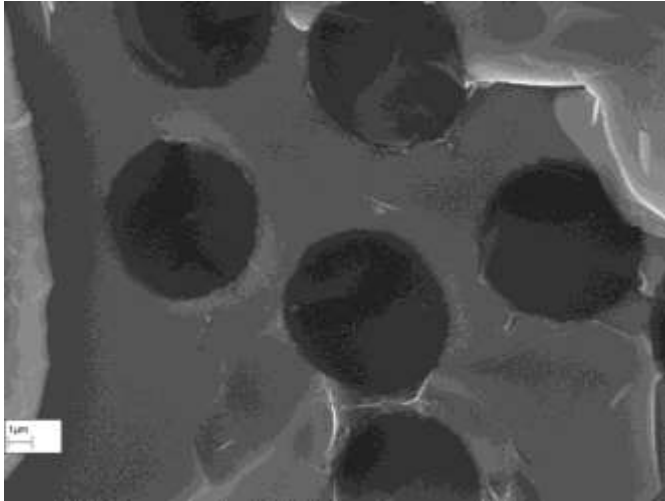
Figure 68 – Fracture surface of the carbon fibers (SEM, SE)
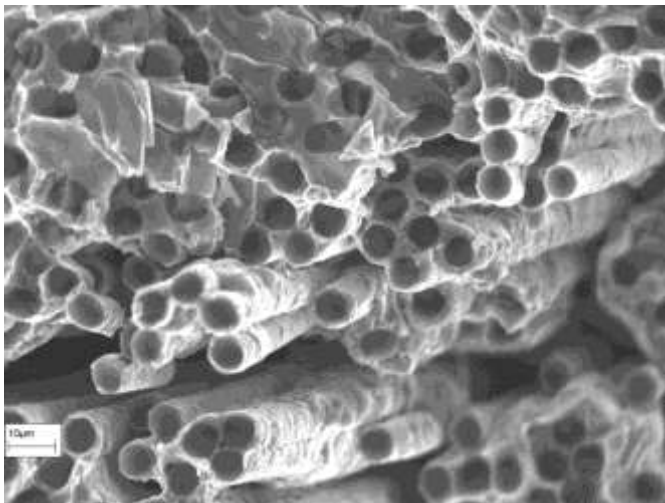
Figure 69 – Fracture surface of fibers that were not completely coated by aluminum (SEM, SE)

4.2.2.2 Energy-dispersive X-ray spectroscopy

The EDX analysis showed that carbon-fiber-reinforced samples presented aluminum-rich intermetallic compounds around the fibers (Fig. 83), what cannot be assured without the support of more precise

examinations concerning chemical and/or crystalline composition. Furthermore, measurements indicate the diffusion of aluminum and/or nickel into the carbon fibers (Fig. 84), what may have led to carbide formation and to embrittlement of the fibers, but requires further tests to be confirmed. Fig. 85 shows the local EDX measurements and Table 11 their correspondent values, that indicate the fibers (Fig. 85 1) remained mostly carbon after que immersion in the melt, but may have reacted with aluminum and nickel (Fig. 85 1 and 2). Fig. 85 3 shows the composition of an intermetallic compound, probably $NiAl_3$ and Fig. 85 4 indicates that the matrix is mainly composed by aluminum.
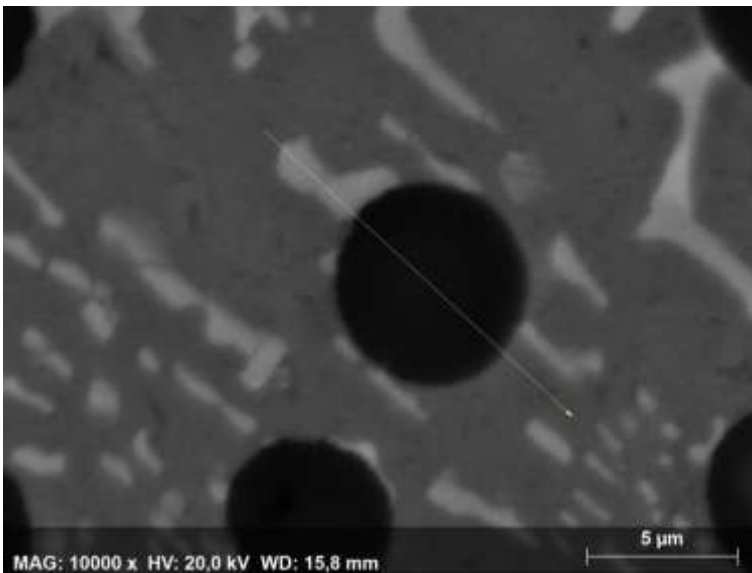
Figure 70 – Line over reinforced sample which was scanned with EDS (SEM, BSE)
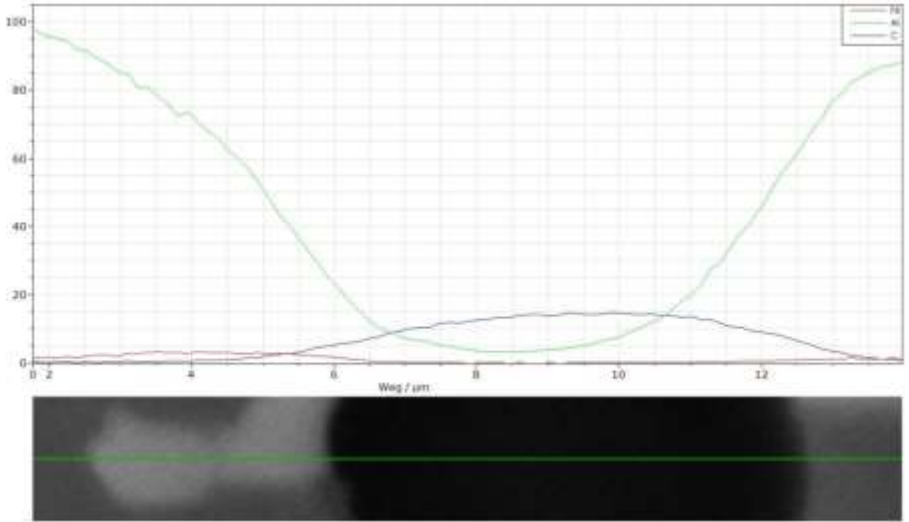
Figure 71 – Qualitative profile of elements over the scanned line
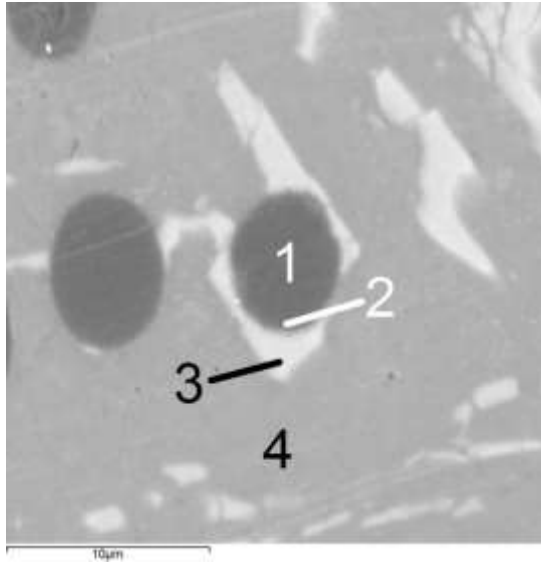
Figure 72 – EDX spot analysis of a sample with fibers

Table 11 – Results of the EDX spot analysis of the sample with fibers

Spot	C (at%)	Al (at%)	Ni (at%)
1	97	3	-
2	94	5	1
3	-	77	23
4	-	99	1

4.2.2.3 X-ray diffractography

As samples with fibers were produced using less nickel, less intermetallic compounds were formed. According to the diffractography (Fig. 86), samples with fibers presented Ni_2Al_3 and NiAl, but also pure aluminum and nickel as well. The formation of nickel carbide (NiC_x) was also identified by the diffractography, meaning the nickel coating of the fibers may have reacted with their substrate, what, even in a small extent, can compromise the reinforcing effect of the fibers through the formation of brittle phases.
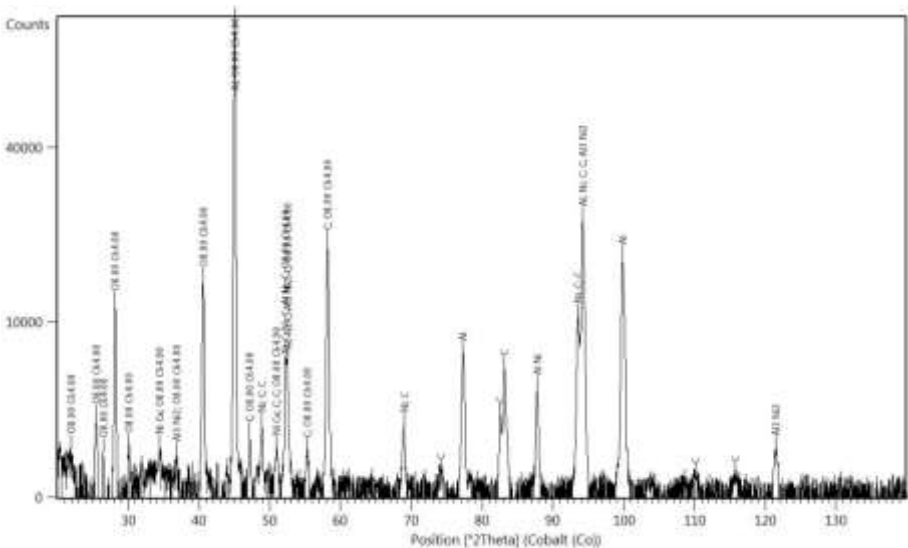
Figure 73 – X-ray diffractography of a sample with fibers after immersion in pure aluminum at 900°C for 15 s

4.2.2.4 Tensile test

A single sample with fibers was tested under tensile, in order to compare with the result of the sample without fibers. The sample presented elastic modulus of 3.8 GPa, yield strength of about 30 MPa, ultimate tensile strength of 55 MPa and elongation of 1.5 % (Fig. 87). The result for the sample without fibers is plotted with a dashed line, for comparison. These results show that the fiber reinforcement decreases the elastics modulus of the composite and can increase yield and tensile strength. However, both properties should be improved and the reason for that not to be verified is that the processing produces samples with high surface roughness, porosity and brittle phase content.
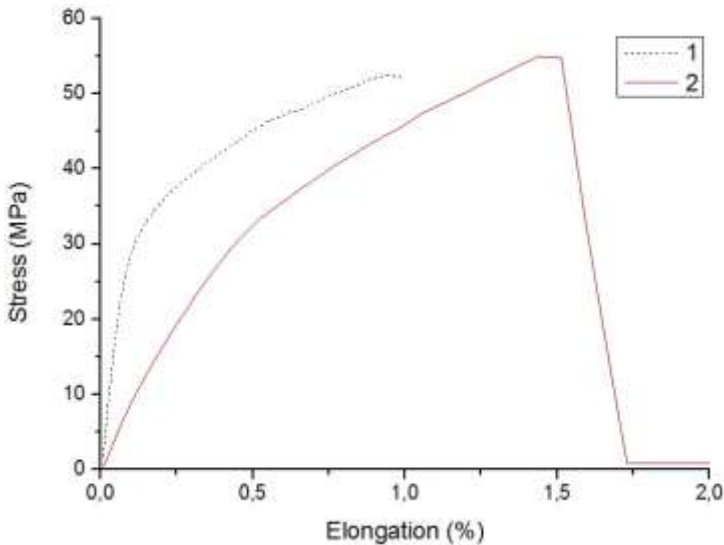
Figure 74 – Tensile test curve for 1 - sample without fibers 2 - sample with fibers

4.2.2.5 4-Point bending test

Reinforced samples presented diverse responses to the bending test (Fig. 88). The heterogeneous distribution of the fibers, the surface roughness and the porosity resulted from incomplete infiltration were responsible for the presence of many deffects in the sample after the immersion in aluminium melt, resulting then in widely scattered values (Table 12). Some influence of the thickness over the strength can be

noticed, since samples with lower fiber content could be better infiltrated by the aluminium melt, leaving less porosity and consequently producing stronger samples. Characteristical strength and Weibull modulus were calculated as 74 MPa and 0.7, respectively. Weibull plot for reinforced samples is showed in Fig. 89.
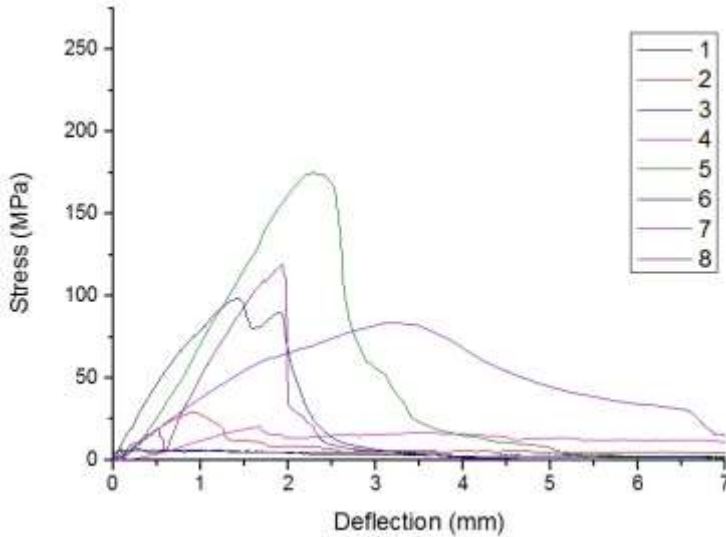
Figure 75 – Bending tests curves for samples with reinforcement

Table 12 – Bending tests results of samples with reinforcement

Sample	Thickness (mm)	Bending Strength (MPa)	Elastic Modulus (GPa)
1	2.3	6	1
2	2.6	29	9
3	2	8	17
4	2.8	20	42
5	1.5	175	40
6	1.5	98	34
7	1.5	84	13
8	1.3	119	50
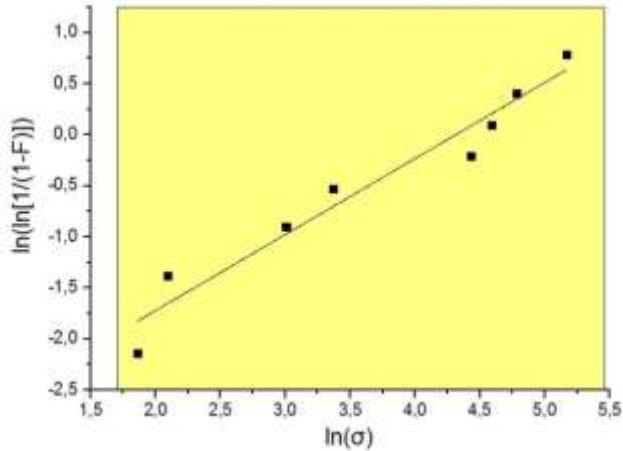
Figure 76 – Weibull plot of the bending tests of samples with reinforcement

4.2.2.6 Fiber content analysis

From overview images of the reinforced samples, for example Fig. 90, the volume fraction of fibers was estimated by the area occupied by the fibers in the picture, after the software Imago binarized it (Fig. 91). Fig. 90 shows a region were infiltration by aluminum melt was successful, forming a massive sample with minor deffects, where the volume fraction of fibers, and by its turn in Fig. 91 (scale bar was cropped off to avoid mismeasurements), was estimated in approximately 15%.
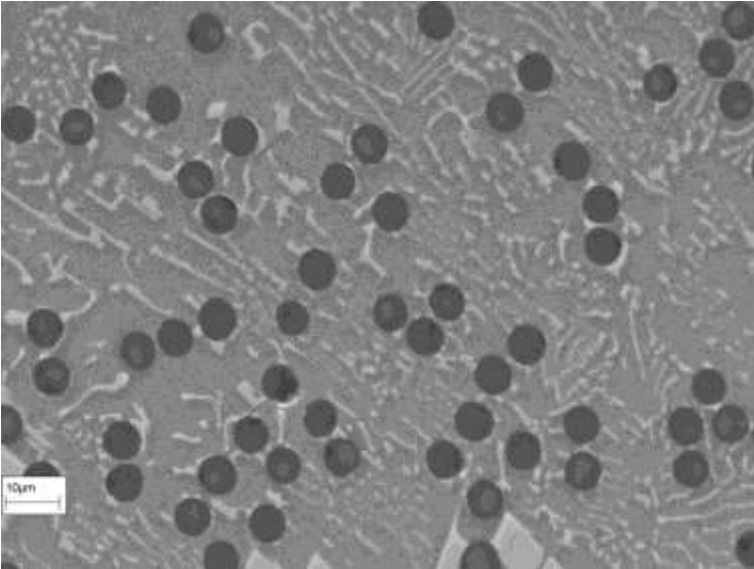
Figure 77 – Reinforced sample picture used to assess the fiber volume fraction (SEM, SE)
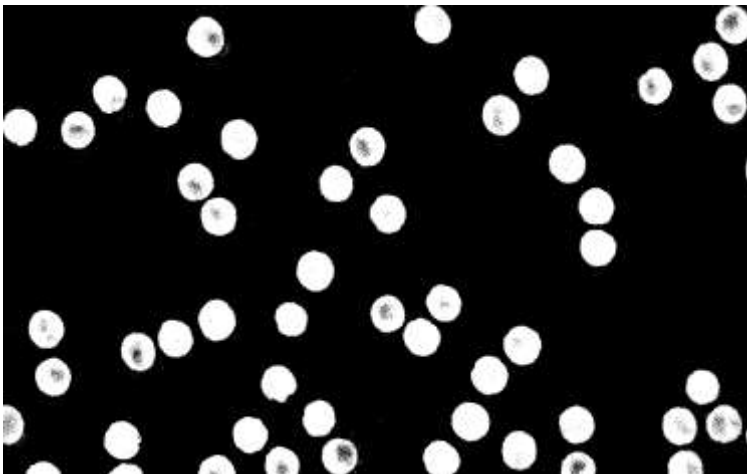
Figure 78 – Binarization of previous figure by the software Imago (white area approx. 15%)

On the other limit, Fig. 92 shows a region of a sample in which fiber concentration was too high for a proper wetting by the aluminum melt, resulting in a microstructure with high density of microcracks. The

Imago analysis (Fig. 93) indicated a fiber volume fraction of approximately 40%. Considering that, at this step of the development, it can be afirmed that fiber content should not exceed 40 vol%.
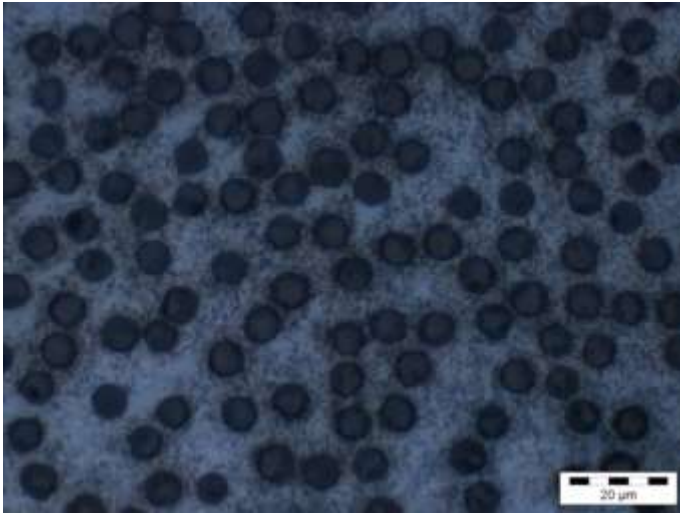
Figure 79 – Reinforced sample picture used to assess the fiber volume fraction (light microscope)

Figure 80 – Binarization of previous figure by the software Imago (white area approx. 40%)

5   CONCLUSIONS AND SUGGESTIONS FOR FURTHER WORKS

5.1   Conclusions

A manufacturing process for the production of carbon-fiber reinforced aluminum matrix composites was designed, by defining a heat treatment for the material to be used as matrix and then adjusting the processing route with a step of fiber incorporation. The process shows much potential for the production of carbon-fiber reinforced aluminum or intermetallic matrix composites.

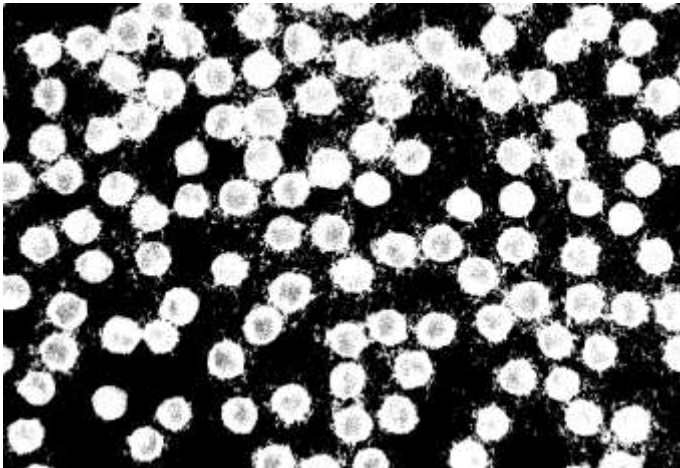The chosen material for the matrix was a cold rolled interlayering of aluminum foils and nickel mesh, aiming further heat treatment with the objective of forming temperature resistant phases. As diffusion, solubilization and precipitation heat treatments did not result in massive samples, immersion in aluminum melt offered the best potential in this work, producing a regular microstructure with different intermetallic compounds (Ni_2Al_3, $NiAl$), which are hard and temperature resistant. On the other hand, these compounds are also brittle, so that their simultaneous growth in multiple directions led to crack formation, decreasing the mechanical properties.

As there was less nickel in the samples with carbon fibers than in the samples without fibers, nickel was almost completely solubilized in those samples, forming a microstructure composed by aluminum matrix, intermetallic precipitates (Ni_2Al_3, $NiAl$) and carbon fibers. The bond between matrix and reinforcement was found to be strong, since fibers broke along the matrix, showing no pull out. However, the high concentration of fibers in some regions of the samples did not allow the aluminum to promote a complete infiltration, so that the remaining porosity caused a large scattering in the mechanical properties of the samples. According to the fiber content analysis, 40 vol% fibers was already a harmful concentration, initiating microcracks, meanwhile 15 vol% resulted in a full wetting of the fibers by the melt and, consequently, strong bonding between fiber and matrix, yet with room for a higher fiber content than 15%.

Since surface roughness could not be removed due to the small thickness and high brittleness of the samples, it might have acted as crack initiator and thus influenced the obtained results for mechanical properties and their scattering, so that the Weibull approach cannot be reliably used in this case.

5.2 Suggestion for further works

Interesting topics for the further development of the manufacturing process of carbon-fiber reinforced aluminum composites could be:

- studying the influence of the mesh size, mesh wire diameter and aluminum foild thickness on the microstructure of cold rolled samples immersed in pure aluminum melt
- evaluating the influence of melt temperature and immersion time in the microstructure of cold rolled samples made of nickel mesh and aluminum foils
- analyzing the microstructure of cold rolled samples made of nickel mesh and aluminum foils after immersion in aluminum melt with different nickel contents
- optimizing the content and distribution of carbon fibers in the composite
- using heat treatable alloys as molten material or produce a heat treatable material through reactive diffusion to form precipitates that would contribute with the fibers for the reinforcement of the composite

REFERENCES

[1] HARRIS, B. **Engineering composite materials**. The institute of materials. 1999.

[2] QURESHI, H. A. Al-. **Materiais compostos – análises e fabricação**. UFSC/CEM. 2010.

[3] MITCHELL, B. S. **An introduction to materials engineering and science**. John Wiley & Sons, Inc. 2004

[4] CALLISTER, W. D.. **Materials Science and Engineering**. 7. ed. John Wiley & Sons, Inc. 2007.

[5] ASHBY, M. F.; JONES, D. R. H. **Engineering Materials 2: An introduction to microstructures, processing and design**. 2. ed. Butterworth-Heinemann. 1998.

[6] FROYEN, L.; VERLINDEN, B.. Aluminum matrix composites materials. **TALAT Lecture 1402**, 1994.

[7] BARTSCH, M. Script for course "Materials for Aerospace Applications" – winter term 2012/13, **Chapter 3. Aeroengines (Jet engines)**.

[8] LAUNEY, M. E.; RITCHIE, R. O. **On the fracture toughness of advanced materials**. Advanced Materials, Vol. 21. 2009.

[9] QIN, Q.; YE, J. **Toughening mechanisms in composite materials**. Woodhead Publishing. 2015.

[10] RICHERSON, D. W. **Modern ceramic engineering: properties, processing and use in design**. 3. ed. Taylor & Francis, 2006.

[11] AVK – INDUSTRIEVEREINIGUNG VERSTÄRKTE KUNSTSTOFFE E. V. **Handbuch Faserverbundwerkstoffe/Composites – Grundlagen, Verarbeitung, Anwendungen**. 4. Auflage. Springer Vieweg. 2013.

[12] CARTER, C. B.; NORTON, M. G. **Ceramic materials: Science and Engineering**. Springer, 2007.

[13] WESSEL, J. K. **Handbook of advanced materials**. John Wiley & Sons. 2004.

[14] Toho Tenax Europe GmbH. **Produktdatenblatt (EU) Tenax® Filamentgarn**. Version 20. 31.08.2015.

[15]   BARTSCH, M. Script for course "Materials for Aerospace Applications" – winter term 2012/13, **Chapter 1. Light weight materials for airframe structures**.

[16]   MALLICK, P.K. **Fiber-reinforced composites – materials, manufacturing, and design**. 3. ed. CRC Press. 2008

[17]   KRENKEL, W. **Keramische Verbundwerkstoffe**. WILEY-VCH Verlag GmbH & Co. KgaA. 2003.

[18]   SGL GROUP – the carbon company – **composite components**. Disponível   em: <https://www.sglgroup.com/cms/international/products/product-groups/cc/index.html?__locale=en>. Acessed on 30th, Oct. 2015.

[19]   PANDEY, A. B.; KENDIG, K. L.; WATSON, T. J. **Affordable metal-matrix composites for high performance applications**. The Minerals, Metals & Materials Society. 2001.

[20]   CLYNE, T. W.; WITHERS, P. J. **An introduction to metal matrix composites**. Cambridge University Press. 1993.

[21]   KAINER, K. U. **Metallische Verbundwerkstoffe**. Wiley-VCH Verlag GmbH & Co. KgaA. 2003.

[22]   CHAWLA, N.; CHAWLA, K. C. **Metal matrix composites**. 2nd ed. Springer-Verlag New York. 2013.

[23]   RICE, R. C.; JACKSON, J. L.; BAKUCKAS, J.; THOMPSON, S. **Metallic materials properties development and standardzation (MMPDS)**. Chapter 3 – Aluminum. National Technical Information Service. 2003.

[24]   LUMLEY, R. **Fundamentals of aluminium metallurgy – production, processing and applications**. Woodhead Publishing. 2011.

[25]   LEYENS, C.; PETERS, M. **Titanium and titanium alloys – fundamentals and applications**. WILEY-VCH Verlag Gmbh & Co. KgaA. 2003.

[26]   DAVIS, J. R. **ASM specialty handbook – nickel, cobalt, and their alloys**. ASM International. 2000.

[27]   ASM Handbook. **Volume 3 – Alloy phase diagrams**. ASM International. 1992.

[28] WESTBROOK, J. H.; FLEISCHER, R. L. **Intermetallic compounds volume 3 – structural applications of intermetallic compounds**. John Wiley & Sons Ltd. 2000.

[29] STOLOFF, N. S.; SIKKA, V. K. **Physical metallurgy and processing of intermetallic compounds**. Chapman & Hall. 1996.

[30] SAUTHOFF, G. **Intermetallics**. VCH Verlagsgesellschaft mbH. 1995.

[31] CAYRON, C. **TEM study of interfacial reactions and precipitation mechanisms in Al_2O_3 short fiber or high volume fraction SiC particle reinforced Al-4Cu-1Mg-0.5Ag squeeze-cast composites**. Thesis (Doctor of Philosophy degree at the Materials Department) – École Polytechnique Fédérale de Lausanne. 2000.

[32] SURAPPA, M. K. **Aluminum matrix composites: challenges and opportunities**. Sadhana. Vol. 28. April 2003.

[33] OLEVSKY, E.; DUDEK, H. J.; KAYSSER, W. A. **Hiping conditions for processing of metal matrix composites using the continuum theory for sintering – I. Theoretical Analysis**. Acta Materialia. Vol. 44. 1996.

[34] OLEVSKY, E.; DUDEK, H. J.; KAYSSER, W. A. **Hiping conditions for processing of metal matrix composites using the continuum theory for sintering – II. Application to fibre reinforced titanium alloys**. Acta Materialia. Vol. 44. 1996.

[35] BETTGE, D.; et al. **Mechanical behavior and fatigue damage of a titanium matrix composite reinforced with continuous SiC fibers**. Materials Science and Engineering A. Vol 452 – 453. 2007.

[36] EVERETT, R.K.; ARSENAULT, R.J. **Metal matrix composites: processing and interfaces**. Academic Press, Inc. 1991.

[37] PORTER, D.A.; EASTERLING, K.E. **Phase transformation in metals and alloys**. 2nd ed. Chapman & Hall. 1992.

[38] SMALLMAN, R.E.; NGAN, A.H.W. **Modern physical metallurgy**. 8th ed. Butterworth-Heinemann. 2014.

[39] ABBASCHIAN, R.; ABBASCHIAN, L.; REED-HILL, R.E. **Physical metallurgy principles**. 4th ed. Cengage Learning. 2009.

[40] Picture from <www.discounter-preisvergleich.de>. Acessed on 8th, Sep. 2015.

[41] Novus Dahle GmbH & Co. KG <http://www.dahle-office.com/produkte/schneidemaschinen.html>. Acessed on 9th, Sep. 2015.

[42] Nabertherm GmbH < http://www.nabertherm.de/produkte/labor/de>. Acessed on 14th, Sep. 2015.

[43] TETZLAFF, U. **Gezielte gerichtete Vergröberung (Floßbildung) des Gamma-Gamma´-Gefüges und Auswirkungen auf die mechanischen Hochtemperatureigenschaften einer einkristallinen Nickelbasis-Superlegierung**. Dissertation Universität Erlangen-Nürnberg. 2000.

[44] GUNT Gerätebau GmbH. **WP 600 Creep Testing Machine – Experiment Instruction**. Available on <http://fetweb.ju.edu.jo/me/courses/labs/materials/Lab_files/Binder_Creep.pdf>. Acessed on 19th, May 2015.

[45] DIN EN 658-3:2002 – Mechanische Eigenschaften von keramischen Verbundwerkstoffen bei Raumtemperatur.

[46] KAWASAKI, T.; et al. **Elastic moduli and stiffness optimization in four-point bending of wood-based sandwich panel for use as structural insulated walls and floors**. The Japan Wood Research Society. Vol 52. 2006.

[47] ESSS <http://www.esss.com.br/index.php?pg=servicos_desenvolvimento_projetos_imago>. Acessed on 15th, Oct. 2015.

[48] HICKL, A.J.; HECKEL, R.W. **Kinetics of phase layer growth during aluminide coating of nickel**. Metallurgical Transactions A. Vol. 6A. 1975.

[49] VOUDOURIS, N.; CHRISTOGLOU, C.; ANGELOPOULOS, G.N. **Formation of aluminide coatings on nickel by a fluidised bed CVD process**. Surface and Coatings Technology. Vol. 141. 2001.

[50] WIERZBA, B.; et al. **The growth kinetics of nickel aluminide coatings by the bi-velocity method**. Chemical Vapor Deposition. Vol. 18. 2012.

[51] RIZOV, B.; MAGDESKI, J. **Interaction of solid nickel with liquid mixture of aluminum and nickel and formation of**

intermetallic phases. Association of Metallurgical Engineers of Serbia. Vol. 16. 2010.

[52] KRASNOWSKI, M.; GIERLOTKA, S.; KULIK, T. **Nanocrystalline Al$_3$Ni$_2$ alloy with high hardness produced by mechanical alloying and high-pressure hot-pressing consolidation**. Intermetallics. Vol. 42. 2013.

[53] WESTBROOK, J.H. **Temperature dependence of hardness of the equi-atomic iron group aluminides**. Journal of the electrochemical society. Vol. 103. 1956.

[54] AZO   Materials <http://www.azom.com/properties.aspx?ArticleID=2193> Acessed on 23rd, Sep. 2015.

APPENDIX

Other approaches on the concept of an aluminum matrix composite performed in this work.

- Interlayering of aluminum foils with nickel coated carbon fibers. Samples were cold rolled at the tips to keep them together. The result was carbon fibers and nickel-aluminum intermetallics precipitates in an aluminum matrix. It is promising, but but it needs something to keep the form, otherwise no sample for mechanical tests can be machined from it.
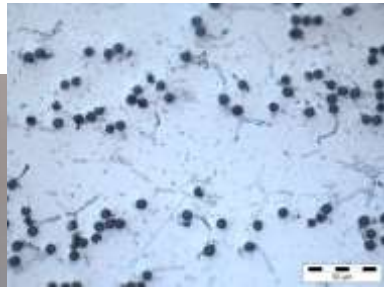
- Production of an aluminum/aluminum oxide laminate by casting aluminum around a ceramic foil. The ceramic foil was too brittle and there was no bonding between it and aluminum.

- Cold rolling of aluminum plates with carbon fibers. Plates were welded by resistance spot welding with carbon fibers between them and then cold rolled. The carbon fibers were destroyed.

- Cold rolling of nickel and aluminum interlayers with ceramic particles. Particles need to be homogeneously distributed a proper ratio between metals and particles needs to be found.